

New insights into the organic carbon export in the Mediterranean Sea from 3D modeling

A. Guyennon¹, M. Baklouti¹, F. Diaz¹, J. Palmieri², J. Beuvier^{3,4},
C. Lebaupin-Brossier⁴, T. Arsouze^{5,6}, K. Béranger⁵, J.-C. Dutay⁷, and T. Moutin¹

¹Aix Marseille Université, CNRS/INSU, Université de Toulon, IRD, Mediterranean Institute of Oceanography (MIO) UM110, 13288, Marseille, France

²Southampton University – National Oceanography Center (NOC), Waterfront Campus, European Way, Southampton SO14 3ZH, UK

³Mercator Ocean, Ramonville Saint-Agne, France

⁴CNRM-GAME, Météo-France/CNRS, Toulouse, France

⁵UME, ENSTA-ParisTech, Palaiseau, France

⁶Laboratoire de Météorologie Dynamique, École Polytechnique, Palaiseau, France

⁷LSCE/IPSL, Laboratoire des Sciences du Climat et de l'Environnement, CEA-CNRS-UVSQ, Gif-sur-Yvette, France

Correspondence to: melika.baklouti@mio.osupytheas.fr

Abstract. The Mediterranean Sea is one of the most oligotrophic regions of the oceans, and nutrients have been shown to limit both phytoplankton and bacterial activities, resulting in a potential major role of dissolved organic carbon (DOC) export in the biological pump. Strong DOC accumulation in surface waters is already well-documented, though measurements of DOC stocks and export flux are still sparse and associated with major uncertainties. This study provides the first basin-scale overview and analysis of organic carbon stocks and export fluxes in the Mediterranean Sea through a modeling approach based on a coupled model combining a mechanistic biogeochemical model (Eco3M-MED) and a high-resolution (eddy-resolving) hydrodynamic simulation (NEMO-MED12). The model is shown to reproduce the main spatial and seasonal biogeochemical characteristics of the Mediterranean Sea. Model estimations of carbon export are also of the same order of magnitude as estimations from in situ observations, and their respective spatial patterns are mutually consistent. Strong differences between the western and eastern basins are evidenced by the model for organic carbon export. Though less oligotrophic than the eastern basin, the western basin only supports 39 % of organic carbon (particulate and dissolved) export. Another major result is that except for the Alboran Sea, the DOC contribution to organic carbon export is higher than that of particulate organic carbon (POC) throughout the Mediterranean Sea, especially in the eastern basin. This paper also investigates the seasonality of DOC and POC exports as well as the differences in the processes involved in DOC and POC exports in the light of intracellular quotas. Finally, according to the model, strong phosphate limitation of both bacteria and phytoplankton growth is one of the main drivers of DOC accumulation and therefore of export.

1 Introduction

The biological pump is recognized as a major component of carbon export in the ocean and plays a significant role in the carbon cycle as a whole (Siegenthaler and Sarmiento, 1993). The sinking of organic particles has long been identified as the main process involved in the biological pump, 25 thereby sustaining the vertical carbon and nutrient gradients in the ocean (Eppley and Peterson, 1979; Sarmiento and Gruber, 2006). Considerable attention has therefore been paid to the export of organic carbon in its particulate form.

Advances in the characterization of dissolved organic pools have led to a better knowledge of the role of the dissolved organic carbon (DOC) compartment in the ocean carbon cycle. As a non- 30 sinking tracer, the fate of DOC is strongly linked to physical processes and its export occurs via vertical mixing and/or downwelling when it lies in intermediate waters, and via oceanic overturning circulation in deep water (Hansell et al., 2002, 2009). If the early works of Copin-Montégut and Avril (1993) in the Mediterranean Sea and Carlson et al. (1994) in the Sargasso Sea were the first attempts to quantify DOC export flux below the euphotic zone, estimation of detrital particulate 35 organic carbon (POC) export began years before with the deployment of sediment traps and isotopics measurements (Buesseler, 1991).

The seasonal variability of DOC in the euphotic zone has been widely recorded in the sub-tropical and temperate areas of the ocean (Carlson et al., 1994; Avril, 2002; Hansell and Carlson, 2001; Santinelli et al., 2013). The results of these studies indicate a time lag between DOC production 40 and consumption, causing summer accumulation in the upper layers due to both biotic and abiotic processes, which either alter DOC bioavailability or reduce bacterial activity. The inefficiency of the microbial loop in organic carbon mineralization - the so-called malfunctioning microbial loop (Thingstad et al., 1997) - induces an accumulation of bioavailable DOC. This inefficiency is directly related to low phosphate availability in the upper waters of the Mediterranean Sea (Moutin et al., 45 2002; Van Wambeke et al., 2002; Thingstad et al., 2005; Santinelli et al., 2013).

In this paper, our aim is to investigate the pathways of organic carbon (OC) at the scale of the Mediterranean Sea, and more specifically to characterize OC export fluxes since this is crucial to determine the efficiency of the biological pump. High resolution 3D modeling using the biogeochemical mechanistic model Eco3M-MED (Aleksenko et al., 2014) forced by the physical model 50 NEMO-MED12 (Beuvier et al., 2012b) was chosen to address this question. Major modeling work has already been done to estimate organic carbon export using box models (e.g. Toggweiler et al., 2003), ocean carbon-cycle models (e.g. Bopp et al., 2001; Sarmiento et al., 1998; Maier-Reimer et al., 1996; Sarmiento and Gruber, 2006) and ecosystem models coupled with hydrodynamic models (e.g. Le Quéré et al., 2010). Several coupled models have also been developed to study the whole 55 of the Mediterranean Sea, starting with the early simulation by Crispi et al. (1998) and Crise et al. (1998). The number of models designed for this purpose is increasing (Lazzari et al., 2013; Mattia et al., 2013; Macías et al., 2014), but to our knowledge, no modeling work has yet focused on or-

ganic carbon fluxes for the entire Mediterranean Sea. Here, our aim is to focus on OC export in the Mediterranean Sea by characterizing and quantifying the associated fluxes, studying their temporal and spatial variability, and providing the first estimations at this scale of the respective contributions of DOC and POC (which refers to the detrital particulate organic carbon only in the present paper) to carbon export. We also aim to analyze the processes involved in DOC and POC production export in the light of the intracellular quotas of planktonic organisms calculated by Eco3M-MED. The paper is organized as follows: After the introduction (Sec. 1), a succinct overview (Sect. 2) of the hydrodynamical model NEMO-MED12 (Sec. 2.1) and the biogeochemical model Eco3M-MED (Sec. 2.2) is provided, given that they are described in detail in the aforementioned papers. Simulation set-up and datasets used for model comparison are also presented. Section 3 first focuses on the results related to organic carbon inventory and export at the scale of the Mediterranean Basin, and for the purpose of discussion results on intracellular quotas in phytoplankton and bacteria as well as on exudation fluxes are also presented. In Sect. 4 results on export are discussed in the context of previous POC and DOC export evaluations in the Mediterranean Sea, and in the light of processes and intracellular quotas in phytoplankton and bacteria. Finally, a Supplementary Material is associated with this paper containing the assessment of the biogeochemical model outputs (nutrients, chlorophyll, primary production and DOC) through comparison with available data and analysis of the main discrepancies.

2 Material and methods

2.1 The hydrodynamic model

The physical run used in this work is described in Beuvier et al. (2012b). It has been simulated by the regional circulation model NEMO-MED12 Beuvier et al. (2012a) which is part of a suite of Mediterranean regional versions of OPA and NEMO (Madec and The-NEMO-Team, 2008) as OPA-MED16 (Béranger et al., 2005), OPAMED8 (Somot et al., 2006) and NEMO-MED8 (Beuvier et al., 2010).

Model resolution is $1/12^\circ$ (≈ 8 km) which means that most of the mesoscale features are explicitly resolved, and the domain includes the whole of the Mediterranean Sea as well as the Atlantic Ocean West of 11°W (Fig. 2). More details of the model and its parametrization are given in Beuvier et al. (2012a).

The simulation was initiated in October 1958 with temperature and salinity data representative of the 1955–1965 period using the MEDATLAS dataset (MEDAR/MEDATLAS-Group 2002, Rixen et al., 2005). Atmosphere forcings are applied daily and come from the ARPERA dataset (Herrmann and Somot, 2008), a 55-year simulation at 50 km and daily resolutions. SST-relaxation and water-flux correction terms, as well as fresh water input from rivers and the Black Sea and Atlantic exchanges are the same as described in Beuvier et al. (2010, 2012a).

2.2 The biogeochemical model

The biogeochemical model Eco3M-MED is embedded in the Eco3M modular numerical tool (Baklouti et al., 2006b), and its structure is similar to the model presented in Alekseenko et al. (2014). Fig. 1 summarizes the interactions between the state variables through the biogeochemical processes. We chose to represent three different element cycles C, N and P in order to reproduce the different limitations and co-limitations observed in the Mediterranean Sea. Silicium, potentially limiting in some regions (Leblanc et al., 2003) is not represented in the model, as P and N limitations are the most common ones in the Mediterranean Sea. Six different planktonic functional types (P.F.T., see Le Quéré et al. (2005) for a proper definition) are represented : 2 primary producers (phytoplankton), 1 decomposer (heterotrophic bacteria) and 3 consumers (nano-, micro- and meso-zooplanktons). The structure of the trophic web thereby includes the main P.F.T.s of the Mediterranean Sea (Siokou-Frangou et al., 2010).

Each P.F.T. of the model is represented through several state variables, namely C, N, P (and Chl for producers) concentrations and a cell number (i.e. an abundance), except for meso-zooplankton which is only represented through its C concentration and its abundance (in individuals per unit volume). Intracellular ratios (i.e. the ratio between two elemental concentrations) as well as intracellular quotas (i.e. the quantity of a given element per cell) can therefore be calculated dynamically by the model. Intracellular ratios are indicators of plankton stoichiometry, i.e. of its C:N:P elemental composition. Early biogeochemical models (NPZD models) have considered a constant C:N:P ratio in plankton given by the canonical Redfield ratio of 106:16:1 (Redfield, 1958). Based on Droop's work (e.g. Droop, 1968, 1975), an increasing number of biogeochemical models (e.g. Baretta et al., 1995; Geider et al., 1998) have in recent decades assumed flexible plankton stoichiometry. Though Droop's original quota function relating growth rate to the intracellular quota of the limiting element was based on cell quotas, these biogeochemical models have used intracellular ratios instead of quotas to regulate the rate of biomass synthesis (and other process rates) with quota functions similar to that of Droop. These flexible stoichiometry models have been widely used in the framework of theoretical batch or chemostat studies (e.g. Geider et al., 1998; Baklouti et al., 2006b) or for large-scale studies with ERSEM (Baretta et al., 1995), BFM (Vichi et al., 2007) or others (e.g. Moore et al., 2002) models. In such models, substrate uptake and biomass synthesis are decoupled, but cell division is not explicitly represented.

Intracellular quotas (or cell quotas) as they are defined in the present paper are indicators of the C, N and P cellular content of plankton. They are an original feature of the Eco3M-MED model in the category of 3D coupled physical-biogeochemical models. This model is based on the assumption that there are a minimum (Q_X^{\min}) and a maximum (Q_X^{\max}) intracellular content for each element X among (C, N, P). Q_X^{\min} can be interpreted as the amount of element X used in cellular structure and machinery, and the accumulated surplus as storage for future growth (Klausmeier et al., 2008). The variability in cell quotas has indeed been widely evidenced through several experimental and in situ

130 studies (e.g. Brown and Harris, 1978; Fukuda et al., 1998; Lovdal et al., 2008; Heldal et al., 2003; Bertilsson et al., 2003; Wilhelm et al., 2013).

The use of cell numbers as state variables and of the associated intracellular quotas offers several advantages: firstly, it makes it possible to distinguish between cell division, which is described by a specific equation, see Eq. 1), biomass synthesis, and uptake. Second, intracellular quotas are indica-
135 tive of the actual internal status of cells, i.e. they indicate whether cells are rich or depleted in a given element, while intracellular ratios only provide relative values. In other words, a given value of intracellular ratio Q_{XY} can correspond to several different cell statuses (for example, a given C:N ratio can be obtained with an infinity of pairs of C and N intracellular concentration values). Thus, intracellular ratios can only provide information on the internal relative quantity of X as compared to that
140 of Y , while intracellular quotas inform on intracellular absolute quantities. The latter information is very useful for the analysis of plankton dynamics since it is informative about the nutritional status of each P.F.T. of the trophic web (see the Discussion section). It is also a good proxy of the quality of the prey available for zooplankton (i.e. whether prey are rich or depleted in a given element). Thirdly, the parameters determined at cell level can be used without using conversion factors. For
145 example, uptake rate measured at cell level (Talarmin et al., 2011), or grazing parameters expressed in number of prey per predator per unit time, such as the ones provided in Christaki et al. (2009) for HNF and ciliates can be used directly.

Intracellular quotas have already been used in previous modeling studies to study phytoplankton growth (Klausmeier et al., 2004) or the dynamics of the planktonic food web (Thingstad et al.,
150 2005). In the latter study, however, cell quotas of carbon were assumed to be fixed in the protozoa, while fixed C:N-ratios were assumed for bacteria and phytoplankton. Moreover, this model was used without being coupled with a physical model (i.e. for the simulation of microcosm and lagrangian experiments).

In the model, the producers are split into two different P.F.T.s according to their theoretical size,
155 i.e. large phytoplankton ($> 10 \mu\text{m}$) mainly encompassing diatoms, and small phytoplankton ($< 10 \mu\text{m}$) which includes picophytoplankton and the remaining nanophytoplankton. The two P.F.T.s have different parameters, distinct predators and fuel different detritic pools (Fig. 1). Decomposers are represented by heterotrophic bacteria and are responsible for the organic matter mineralization, including hydrolysis of particles. Zooplankton is divided into three different size groups, heterotrophic
160 nanoflagellate (HNF) which feeds on bacteria and small phytoplankton, ciliate which feeds on small phytoplankton and HNF, and mesozooplankton (copepods) which feeds on ciliate, HNF and large phytoplankton. Copepods are the only metazoans in the model, and mechanisms such as individual growth, egg production or reproduction are implicitly represented (Alekseenko et al., 2014).

The processes used in the model are extensively described in the aforementioned reference. How-
165 ever, for the purposes of the present paper, we recall that POC is fueled by the natural mortality of largest organisms (mesozooplankton, diatoms and ciliates) and by the egestion of fecal pellets and

sloppy feeding by mesozooplankton, and consumed by POC hydrolysis to DOC. The DOC pool has many inputs (phytoplankton exudation, zooplankton excretion, mortality of small organisms, POC hydrolysis) and a single output (uptake by bacteria). The formulations of most of the biogeochemical processes, for which details are extensively given in Baklouti et al. (2006a, 2011); Mauriac et al. (2011), and Alekseenko et al. (2014), follow cell level mechanistic considerations. Intracellular ratios (Q_{XY}) and intracellular quotas (Q_X) are used to regulate growth via Droop's quota function (Droop, 1968) and net uptake and grazing rates via Geider's limitation formulation (Geider et al., 1998). For example, the specific growth rate (i.e. the division rate) μ of all unicellulars in the model is given by the following equation:

$$\mu = \mu^{\max} \min_{X \in \{C, N, P\}} \left(1 - \frac{Q_X^{\min}}{Q_X} \right) \quad (1)$$

where μ^{\max} is the maximum division rate and Q_X^{\min} the minimum intracellular X quota.

Grazing, primary production and uptake rates are controlled firstly by the organism's environment (either prey or nutrient concentration, or light availability). Secondly, the internal cell status represented by intracellular quotas and ratios drives a feedback regulation of the net incorporated biomass through quota functions. Hence, the uptaken surplus (which becomes more and more significant as the intracellular quota approaches Q^{\max}) is either released in its initial form or exuded in the form of DOM. In the same way, excretion and fecal pellet production fluxes are proportional to the grazing flux and to a quota function the value of which increases as the quota approaches Q^{\max} . Furthermore, 10 % of the material grazed by mesozooplankton directly fuels the particulate organic matter stock, to represent sloppy feeding. Respiration rates are estimated via energy costs for every plankton activity (Alekseenko et al., 2014). Nitrification is represented through first order kinetics while particulate hydrolysis function depends on bacteria intracellular quotas (POC hydrolysis increases with bacterial C-limitation). Grazing by higher trophic levels is implicitly taken into account via quadratic mortality affecting only mesozooplankton. Grazing function is a Holling II type (Holling, 1959; Kooijman, 2000) for multiple prey. The only difference with the configuration of Alekseenko et al. (2014) lies in the formulation used to represent predator preferences for multiple prey. We here used the "Kill The Winner" (KTW) formulation depicted in Vallina et al. (2014), which combines active-switching (i.e. the preference of a predator for a given prey depends on prey density) and an ingestion rate always increasing with the total biomass of prey. This active-switching formulation was used to preserve foodweb diversity (e.g Prowe et al., 2012) and to prevent unrealistic predator-prey oscillations.

Since the model relies on a mechanistic basis, parameters are mainly physiological (and measurable) and they were either taken from literature or derived from other parameters on the basis of physiological considerations and in the interests of greater consistency between parameters. For example, maximum intracellular quotas are inferred from minimum ones as done in Thingstad et al.

(2005). Another example lies in the relationship between the maximum uptake rate of a given element, which is the product of the maximum specific growth rate and the maximum intracellular quota in that element. Other examples as well as the whole set of parameters are given in Alekseenko et al. (2014).

2.3 Model coupling

The models NEMO and Eco3M-MED have been associated for the first time. The coupling between the hydrodynamic and biogeochemical models is offline, i.e. biological retroaction on the physics is not taken into account. Daily-averaged water velocities were used for the advection of biogeochemical tracers, using a MUSCL scheme (horizontal and vertical diffusion fluxes are calculated according to a centered scheme). The time-step used for the numerical integration of the tracer conservation equations equals 1200 s. A sinking velocity of 2 m d^{-1} is applied only on the particulate organic pool (i.e. the detrital compartment). The aim of this compartment is to represent particles with different sizes and sinking velocities and the value of 2 m d^{-1} is within the usual range found in the litterature (Vichi et al., 2007; Fasham et al., 2006). Light attenuation formulation in the water column is based on Morel (1988) results.

2.4 Initial and boundary biogeochemical conditions

Initial nutrient and chlorophyll fields are derived from annual means of Mediterranean Sea climatological data (Schaap and Lowry, 2010). The remaining biogeochemical variables are derived from chlorophyll using conversion factors derived from published works (see Alekseenko et al. (2014) for details).

A "buffer-zone" has been defined between the domain western boundary and the Gibraltar Strait (from 11°W to 6°W), in which a damping procedure towards Atlantic conditions has been applied. The restoring time is 2 days west of 7.5°W , linearly increasing to 90 days from 7.5°W to 6°W (Fig. 2). Atlantic nutrient concentrations come from the World Ocean Atlas monthly climatology (Garcia et al., 2006), so that the nutrients damping in the "buffer-zone" takes into account the nutrients' monthly variability. Given the inaccuracies in phosphate measurements, we decided to compute phosphate profiles from that of nitrate by imposing a redfield ratio of 16 in order to be more consistent with observed $\text{NO}_3:\text{PO}_4$ ratios in this region (Gómez, 2003). Chlorophyll concentrations were not provided in this database. We therefore used in situ data from the SeaDataNet database to create a mean vertical chlorophyll profile for the Atlantic, and then used a climatology of surface chlorophyll from the GlobColour product in this region to represent an annual cycle of the chlorophyll vertical profile. The remaining Atlantic biogeochemical variables were derived from chlorophyll using the same procedure as for initial conditions.

Nutrient (NO_3 and PO_4) inputs from riverine influx and coastal runoffs are derived from Ludwig et al. (2009), following the same procedure as for the riverine freshwater inputs in the circulation

model (Beuvier et al., 2010, 2012b). The nutrient influx of the 29 rivers included in the RivDis database (Vörösmarty et al., 1996) are taken into account in the simulation, while the nutrients of the remaining rivers from the Ludwig et al. (2009) database are averaged for every sub-basin and distributed along their respective sub-basin's coast as coastal runoffs. Dissolved organic carbon inputs in the Mediterranean Sea are distributed in every sub-basin according to the riverine DOC estimates of Ludwig (1996) (a total of $\sim 1.8 \text{ Tg C y}^{-1}$ in the whole of the Mediterranean Sea). Sub-basin DOC inputs were then distributed among fluvial estuarine and coastal runoffs to match circulation model freshwater geographical distribution (Palmiéri, 2014; Palmiéri et al., in prep).

Mass exchanges with the Black Sea in the Dardanelles Strait are treated as river inputs, with nutrients and DOC input concentrations provided by the SESAME project (Tugrul and Besiktepe, 2007; Meador et al., 2010). But, since NO_3 budget indicates a negative net flux of NO_3 the Dardanelles Strait (i.e. exiting from the Mediterranean), NO_3 flux at Dardanelles is set to zero and the outcome is transferred on the Aegean sub-basin's runoffs. These runoffs are artificially reduced in order to keep the riverine budget of NO_3 in the Aegean sub-basin realistic.

2.5 Simulation set-up

Using the biogeochemical initial conditions defined in Sect. 2.4, we have conducted a 5 years simulation using physical forcings from the years 1973-1977. This first simulation was considered as a 'spin-up', in order to reduce the impact of state variables adjustment in the simulations. It has deliberately been done long enough before the Eastern Mediterranean Transient period (starting around 1991) which is not stable enough to be chosen as a spin-up period. Moreover, due to high computational costs, it was not possible to run this first simulation until the year 1996. We therefore used the final biogeochemical state of this spin-up as initial conditions for a second simulation running from 1996 to 2012. In this second simulation, only the years following 1998 are considered, since the first 3 years were treated as an additional spin-up beyond which the stability of the run was ensured (i.e. no drift could be observed).

2.6 Data description

The aim of the present work is to study and to quantify organic carbon export fluxes using a 3D physical-biogeochemical model. For this purpose, our first aim was to assess the reliability of our model by examining the agreement between different model outputs and corresponding available data : chlorophyll, nutrients, DOC concentrations and primary production rates.

Three type of comparisons were undertaken : (i) at basin scale, using surface chlorophyll fields provided by satellite for comparisons (ii) at basin scale, using BOUM cruise transect as a "snapshot" to compare nutrients and DOC vertical profiles during the stratified period (iii) at a local scale using the time series data collected at DyFaMed station

2.6.1 Chlorophyll data derived from satellite

Among the specificities of the Mediterranean Sea, its strong oligotrophy and the major influence of colored dissolved organic matter, make the use of classical satellite chlorophyll products difficult (e.g. Claustre et al., 2002). Several algorithms have already been developed (Bosc et al., 2004; 275 D'Ortenzio et al., 2002; Volpe et al., 2007), using different satellite reflectances and datasets. Here, we used a daily surface chlorophyll product delivered by the Myocean project (<http://www.myocean.eu>). In this product, chlorophyll concentrations have been derived using the MEDOC4 algorithm developed by Volpe et al. (2007). This algorithm was built using a large dataset of chlorophyll concentrations collected in situ and reflectance measurements from 3 satellites (Seawifs, MERIS and 280 MODIS), constituting a homogeneous series from September 1997 to March 2012.

2.6.2 The BOUM cruise data

The BOUM cruise took place during summer 2008 (from June 16 to July 20) and traversed both the western and eastern basins of the Mediterranean Sea (Moutin et al., 2012a). The data acquired during this cruise provide a unique picture of the biogeochemical status of the Mediterranean Sea since 285 many biogeochemical variables were observed. Measurements of nutrients and DOC concentrations were used to perform a basin-scale comparison during the summer stratified period with the model outputs obtained at the same dates as the cruise, and averaged over this period.

2.6.3 The DyFaMed station data

The DyFaMed station is located in the Ligurian Sea at 7.9°E and 43.4°N (Fig. 2) and is isolated 290 from coastal inputs by the Mediterranean Northern Current. A strong winter mixing is observed in this area, although it is less intensive than the deep convection occurring in the Provencal sub-basin (Marshall and Schott, 1999). Nutrients (Pasqueron de Fommervault et al., 2015), chlorophyll (Marty et al., 2008), dissolved organic carbon (Avril, 2002) and primary production rates (Marty et al., 2008) time series were used for comparison. The comparison of the model outputs with DyFaMed 295 time series can be done through different methods. The simplest consists in using a single grid point which is the nearest to the DyFaMed station location. This implies that the model perfectly reproduces spatial patterns in this region, which is obviously never the case. On the other hand, the use of model outputs averaged on several grid points around the DyFaMed station amounts to dampening signal variability. We finally chose to use the nearest gridpoint to the DyFaMed station, 300 while assessing spatial variability in the 8 neighbouring grid points (see Supplementary Material).

3 Results

3.1 Organic carbon inventory and export

3.1.1 Dissolved organic carbon inventory

In the following section, mDOC refers to the modeled dissolved organic carbon integrated over the first 100 m of the water column. Seasonal variations of mDOC are given in Fig. 3. Low mDOC values ($< 1 \text{ mol m}^{-2}$) are observed throughout the year in the Alboran Sea (and up to the Balearic Islands), the North Levantine basin, and in some well marked structures in the Tyrrhenian Sea. In contrast, very high mDOC values (up to 5 mol m^{-2}) can be found throughout in the North Adriatic Sea and along the Lybian Coast. Apart from these regions, mDOC is low everywhere (below 2 mol m^{-2}) in winter (Fig. 3 a), and this is also true in spring except in the region of the spring bloom in the Provencal sub-basin. In the western basin, highest DOC concentrations are generally observed in summer, with values reaching 4 mol m^{-2} in the bloom region of the Liguro-Provencal sub-basin. In the eastern basin, they are reached in autumn and mostly concern the Adriatic Sea, and the regions along the southern and eastern coasts.

3.1.2 Particulate organic carbon inventory

In what follows, mPOC refers to the modeled particulate organic carbon integrated over the first 100 m of the water column. Seasonal variations of mPOC are given in Fig. 4. Unlike mDOC, mPOC highest values are observed in winter and spring. This is mostly true for the western basin since, in the eastern basin, mPOC remains low ($< 0.05 \text{ mol m}^{-2}$) all over the year, except for the Adriatic Sea and a local maximum in the Rhodes Gyre distinguishable in spring. During winter (Fig. 4 a), the highest values of mPOC ($> 0.5 \text{ mol m}^{-2}$) are found in the region of the Alboran Sea and the surrounding Balearic Islands and also in the Liguro-Provencal sub-basin though with much lower concentrations. In the Adriatic Sea, mPOC is in the range $[0.1;0.2] \text{ mol m}^{-2}$. Elsewhere, mPOC is low ($< 0.2 \text{ mol m}^{-2}$). During spring (Fig. 4 b), the maximum mPOC is observed in the region of the bloom in the Provencal sub-basin ($\approx 0.4 \text{ mol m}^{-2}$) and the North Adriatic Sea. During summer and autumn (Fig. 4 c and d), overall values are low ($< 0.05 \text{ mol m}^{-2}$), except in the Alboran Sea (where values reach 0.3 mol m^{-2}) and in the North Adriatic Sea.

3.1.3 Dissolved and particulate organic carbon export

Organic carbon fluxes are computed by adding the contribution of advection (vertical velocity and settling velocity for POC) and vertical diffusion (implicitly representing turbulent and convective mixing) fluxes across an horizontal section of the grid. Negative fluxes account for downward fluxes. For clarity, modeled fluxes will be referred to as F_{DOC} , F_{POC} and F_{OC} as the sum of the latter two. F_{DOC} and F_{POC} have been computed at 100 m and 200 m so as to include most of the productive

layer and to allow the comparison in space and time between regions. These depths are also used in
335 several other modeling studies (Lévy et al., 1998; Bopp et al., 2001).

The yearly amount of mOC export at 100 m is equal to 48.4 MtC y^{-1} . The eastern basin is the
main contributor to this export with a total export of 28.7 against 19.7 MtC y^{-1} for the western
basin. mDOC export is equal to 38.8 MtC y^{-1} , and comparatively, river inputs of mDOC are equal
to 1.8 MtC y^{-1} , thereby representing less than 5% of the exported mDOC. mDOC contribution to
340 the total organic carbon flux is dominant. In the western basin, the total amounts of exported mPOC
and mDOC below 100 m are respectively 7.0 MtC y^{-1} and 12.7 MtC y^{-1} , meaning that 64 % of
this export is due to DOC. In the eastern basin, DOC is responsible for 90 % of the organic carbon
export below 100 m, with an annual flux of 26.1 (against 2.6 for POC) MtC y^{-1} .

3.1.4 Spatial variability of export fluxes

345 Mean F_{OC} over the whole basin equals $-22.8 \text{ gC m}^{-2} \text{ y}^{-1}$, but a wide spatial variability can be
observed in Fig. 5. Hence, the main regions of mOC export are the Liguro-Provencal sub-basin, the
Alboran Sea, the southern continental slopes and the Adriatic Sea.

In the western basin, high positive values (i.e. upward) of F_{DOC} are simulated along the French
and Spanish coasts, the entrance to the Sicilian Strait and north-eastern Excluding these areas, the
350 highest downward fluxes of DOC are calculated in the Provencal sub-basin (especially in the region
of deep convection), the north of the Balearic Islands and along the Algerian slope, where downward
 F_{DOC} can be higher than $60 \text{ gC m}^{-2} \text{ y}^{-1}$.

In the eastern basin, the complexity of topography and hydrodynamic regimes in the Aegean
Sea may explain the high heterogeneity of the fluxes calculated in this region that are difficult to
355 interpret. Highest downward F_{DOC} values are located along the continental slope from the Libyan
to the Turkish coasts and in the Adriatic Sea. Elsewhere (i.e. in the open sea), F_{DOC} distribution is
more homogeneous, with a median of $-17 \text{ gC m}^{-2} \text{ y}^{-1}$.

A strong difference exists between the western and eastern basins regarding F_{POC} at 100 m.
The mean value of downward F_{POC} throughout the western basin is $-9.8 \text{ gC.m}^{-2}.\text{y}^{-1}$ against -2.4
360 $\text{gC m}^{-2} \text{ y}^{-1}$ in the eastern basin (Fig. 5 bottom).

In the western basin, F_{POC} is the highest in the Alboran Sea, particularly in the south east of
the easily identifiable anticyclonic eddies. Following the pathway of the Atlantic waters, downward
 F_{POC} values decrease to reach absolute values lower than $5 \text{ gC m}^{-2} \text{ y}^{-1}$ in the Tyrrhenian Sea. In
the Provencal basin high POC fluxes linked to the deep convection, with values ranging from -15
365 to $-30 \text{ gC m}^{-2} \text{ y}^{-1}$ have been modeled. Throughout the eastern basin, F_{POC} is low except in the
Adriatic Sea.

Finally, as suggested in Fig. 5, the spatial correlation between POC and DOC fluxes is weak almost
everywhere. Regions of high POC or DOC export generally do not match. The only areas associated

with both high POC and DOC exports are the Algerian coast, the Adriatic coast, the regions of deep
370 convection and a band east of the Balearic Islands.

3.1.5 Seasonal variability

The seasonal variability and the spatial distribution of F_{DOC} and F_{POC} differ significantly (Fig. 6
and 7). In winter (Fig. 6a), F_{DOC} values are high in almost all of the Mediterranean Basin except
the Alboran Sea, with maximum values that can be observed in the Provencal sub-basin and along
375 the continental slopes, especially along the southern and eastern coasts of the eastern basin. F_{DOC}
distribution is quite similar in autumn, though with values that are significantly lower everywhere.
During the rest of the year, F_{DOC} values are very low in spring nearly everywhere, and almost
null in summer. In several areas (Tyrrhenian and Adriatic Seas, Levantine and Ionian basins), high
downward F_{DOC} values are observed in winter while they are almost null during the rest of the year.

380 High downward POC fluxes at 100 m were calculated from winter to spring west of 7°E, namely in
the Alboran Sea and the Provencal sub-basin (Fig. 7). In these regions, maximum values are reached
in late winter (February-March) in the Alboran Sea, and in spring (March-April) in the Algerian
Sea and the Provencal sub-basin. POC export in the eastern basin (excluding the Adriatic Sea) is
very weak (even in the Rhodes Gyre) all year long. Maximum values can however be identified in
385 spring in the Tyrrhenian Sea, the Levantine basins (except for the Rhodes Gyre where the maximum
is earlier in winter) and in the Adriatic Sea.

3.1.6 Export below 200 m

Below 100 m, organic carbon is progressively consumed via the bacterial activity and respiration.
At 200 m, the calculated mean export fluxes of total organic carbon are reduced by almost 87 % and
390 64 % compared to those at 100 m, respectively in the western and eastern basins. However, the ratio
between export at these two depths is highly variable, depending on the region (see Fig. 8).

For POC (Fig. 8 a), if we consider first the regions where the annual F_{POC} values are significant,
i.e. west of 7°E, (see Fig. 5 bottom), the 200 m to 100 m ratio is lower than 0.25 (i.e. only 25 % of
the carbon exported at 100 m goes below 200 m) in a region including the Alboran Sea, the western
395 Algerian Sea and the Balearic Sea. This ratio is slightly higher but still below 0.3 for the central
Algerian Sea and the Adriatic Sea. The Provencal sub-basin is the only region of high export below
200 m with a ratio about 0.4. In regions of low annual POC export (i.e. east of 7°E), the ratio ranges
between 0.4 and 0.8 in the Tyrrhenian Sea, the Ionian and Levantine basins.

For DOC (Fig. 8 b), the ratio is more spatially variable, and in some regions the ratio is higher than
400 0.4, namely in the Provencal sub-basin, along the coasts of the Levantine basin, in the North Ionian
basin, the Rhodes Gyre and the Adriatic Sea. Some patches of high ratios are also visible close to
the Algerian Coast. Elsewhere the ratio ranges from almost zero (Tyrrhenian Sea, the Alboran Sea)
to 0.2 in the eastern basin.

3.2 Intracellular quotas in bacteria and phytoplankton

405 Intracellular quotas in phytoplankton and bacteria are required for a further analysis of POC and DOC export fluxes and are presented in the following section. Carbon quota (Q_C) in small phytoplankton is maximum (> 0.7) in spring and summer in almost all of the Mediterranean Sea, though Q_C values are slightly lower in spring than in summer in the western basin, especially in the bloom region (Fig. 9). In autumn, though Q_C has decreased in nearly all of the Mediterranean Sea, Q_C values along the southern and eastern coasts of the eastern basin are significantly higher than in the rest of the open sea. In winter, Q_C values are even lower, with local maximum located in the Balearic Sea and in the south of the eastern basin.

The seasonal signal of the P quota (Q_P) in small phytoplankton is nearly the opposite of that of Q_C values in autumn and mostly in winter in nearly the whole of the Mediterranean Basin, and the lowest ones in spring and summer (Fig. 10). All year long, Q_P values are lower along the southern and eastern coasts than in the rest of the eastern basin.

Bacteria Q_C generally increases from winter to summer in most of the Mediterranean Basin (Fig. 11). In autumn, the decrease in Q_C is observed everywhere except throughout the same already identified region (namely along the southern and eastern coasts of the eastern basin). All year round, Q_C values are higher in this region than in the rest of the basin and even reach the Q_C^{\max} value in summer and autumn thus indicating that carbon needs for bacteria growth are fully satisfied. In the deep convection regions (Liguro-Provencal sub-basin, Adriatic, Rhodes Gyre region), and in some eddies well identified in the Alboran and Tyrrhennian seas, the carbon quota is generally lower than in the surrounding waters, especially in autumn.

425 Bacteria Q_P values are very low everywhere in spring and summer except in the latter regions. The minimum Q_P values (i.e. the highest bacterial P-limitation) are observed in spring in the western basin, while they are reached in summer in the eastern basin. As for phytoplankton, Q_P values are lower all year round along the southern and eastern coasts than in the rest of the eastern basin.

3.3 DOC exudation by phytoplankton

430 DOC exudation by large phytoplankton mainly occurs in the bloom region of the western basin (especially in the deep convection zone), in (late) winter and spring where accumulated fluxes are up to 2.8 mol C.m^{-2} (Fig. 13). Elsewhere, exudation fluxes are very low throughout the year, except in the Alboran Sea, two eddies of the Adriatic Sea and in the Rhodes gyre region.

The seasonality and the spatial patterns of DOC exudation flux by small phytoplankton are rather different. The highest mDOC exudation fluxes are modeled in spring in the western basin, especially in the Gulf of Lions and the deep convection zone where accumulated fluxes up to 3 mol C.m^{-2} are calculated. In the eastern basin, the highest fluxes are observed in spring and summer. During these seasons, apart from the Adriatic Sea (especially in the north and along the eastern coast

where accumulated fluxes also reach 3 mol C.m^{-2}) and some hot spots (Rhodes gyre, Nile plume),
440 mDOC exudation seems homogeneous though a north-south gradient is present. Hot spots of mDOC
exudation are also present nearly all year long in the plumes of the main rivers.

4 Discussion

4.1 The dissolved fraction in the organic carbon export is predominant at the scale of the Mediterranean Sea

445 One of the main results of this study is that mDOC export exceeds mPOC export in the whole of the Mediterranean Basin, with the exception of the Alboran Sea (west of 3°W). This is consistent with the comparisons between POC and DOC exports performed in the Tyrrhennian, North Ionian and Ligurian seas by Copin-Montégut and Avril (1993); Santinelli et al. (2013) or by Lefèvre et al. (1996) who estimated that DOC was the main source of remineralization processes in the aphotic
450 layer. In the western basin, the ratio of mDOC over mPOC export fluxes ranges between 2 and 5, and is approximately equal to 4 at the DyFaMed grid point. Observations at the DyFaMed station led to a oDOC export estimation of about 11.9 gC m⁻².y⁻¹, markedly higher than oPOC export estimations at 200 m (Avril, 2002, and references herein). Moreover, oPOC fluxes calculated by Miquel et al. (2011) during the 2001-2005 period ranged from 1.6 to 2.6 gC m⁻².y⁻¹. For comparison, mPOC
455 export flux was in the range [1.5;3.1] gC m⁻².y⁻¹ during the same period. In the northwestern basin, the modeled ratio is about 2 at 100 m and 200 m, while in the same area a modeling study (Herrmann et al., 2014) led to a ratio at 200 m which ranged from 0.9 to 1.8, even though the corresponding export fluxes were higher than in the present study.

The ratio between modeled DOC and POC exports at 100 m ranges from 2 to 8 in the Adriatic
460 Sea. In the same region, a oDOC flux of 15.4 (against 23 for mDOC) gC m⁻².y⁻¹ was estimated from observations by Santinelli et al. (2013). This is nearly 5 times higher than the measured oPOC export flux estimated by Boldrin et al. (2002) under the euphotic zone of 3.3 (against 4.5 for mPOC export at 100 m) gC m⁻².y⁻¹. These oDOC and oPOC fluxes were however estimated at different periods.

465 In the eastern basin, mDOC export is regularly more than 10 times that of mPOC, due to the very weak mPOC export and to the high mDOC export along the coasts and in the open sea. Few observations and estimations are available for this region. In the northern Ionian Sea, Boldrin et al. (2002) reported annual oPOC fluxes at 150 m of 2.4 gC m⁻².y⁻¹, which are in the same order of magnitude as the annual mPOC fluxes calculated in the same area but for a different period (1.2 gC
470 m⁻².y⁻¹ and 0.6 gC m⁻².y⁻¹ at 100 m and 200 m, respectively).

DOC predominance in the OC export flux is first due to the higher DOC gross production fluxes as compared to those of POC, and this still holds if the POC to DOC hydrolysis flux is ruled out (i.e. if the DOC inputs due to POC hydrolysis are not taken into account). At the scale of the Mediterranean Basin as a whole, mDOC and mPOC gross production fluxes are indeed respectively equal to 20
475 10¹² and 2.7 10¹² molC.y⁻¹. In the western basin, mDOC predominance in the export of OC still holds though to a lesser extent, with mDOC and mPOC gross production fluxes respectively equal

to $8.7 \cdot 10^{12}$ and $1.9 \cdot 10^{12} \text{ molC.y}^{-1}$. In the following section, the reasons for these differences will be further analyzed in the light of the processes associated with DOC and POC production.

4.2 POC and DOC exports are characterized by different processes and timing

480 Strong disparities can be identified between the spatial patterns of the annual DOC and POC export fluxes (figure 5), with rather homogeneous DOC export fluxes across the Mediterranean Sea (though with well identified regions of maximum export that will be analyzed later), contrasting with the high east-west gradient in POC export. This is consistent with in situ measurements of daily POC export across the Mediterranean Sea at 200 m that showed much lower POC export in the eastern
485 basin than in the western basin (Moutin and Raimbault, 2002).

There are also considerable differences in the seasonality of DOC and POC export fluxes (Fig. 6 and 7). Over the whole of the Mediterranean Sea, 88 % of DOC export occurs between November and February, which is consistent with observations at the DyFaMed station where 90% of annual DOC export was linked to winter mixing (Avril, 2002). By contrast, POC export is more even
490 throughout the year, and during the same period only 23 % of POC is exported.

In the model, only the detrital compartment (POC) is allowed to sink. The sinking process is therefore the only source of explicit distinction between POC and DOC exports, but it is probably not sufficient to explain the strong aforementioned differences. The main source of difference lies in the biogeochemical processes that fuel or consume POC and DOC pools (see section 2.2). In the
495 model, POC is fueled by the natural mortality of the largest organisms (mesozooplankton, diatoms and ciliates) and by the egestion of fecal pellets and sloppy feeding by mesozooplankton. Thus, higher concentrations of large organisms in the western basin, primarily due to the spring bloom in the Liguro-Provençal sub-basin associated with high primary production rates is the main reason for the higher POC production and export in this basin. Hence, POC export is at a maximum in spring
500 (i.e. from March to May in figure 7) since it is the period including the maximum and the end of the bloom during which detrital concentrations of large organisms are highest. Moreover, according to the model, mortality is the main process that fuels the POC pool, far ahead of the egestion and sloppy feeding processes. More generally, a strong correlation between annual primary production and POC export has been evidenced at basin scale (Spearman's rank correlation coefficient is 0.84),
505 while this is not the case for DOC export (correlation below 0.01).

As shown in the Results section, the regions of high POC or DOC export are generally not the same, except for the regions characterized by high primary production rates during the spring bloom, namely the Alboran Sea, the bloom region in the NW Mediterranean Sea and the south of the Adriatic Sea (see also section 4.3). Apart from these regions, the annual DOC export at 100 m is relatively
510 high in almost all of the Mediterranean Basin, particularly in autumn and winter, and is the consequence of DOC accumulation in the 0-100 m layer during summer and autumn (Fig. 3). DOC export

does indeed take place when DOC rich surface waters plunge or are mixed with poorer deeper waters.

This accumulation of DOC is primarily due to water stratification that results in nutrient depletion in the 0-100 m layer. As a result, the pool of DOC in phytoplankton is saturated with newly synthesized organic compounds since photosynthesis (i.e. carbon production), which is not controlled by P-availability, takes place more rapidly than is required to supply the needs of growth (cell division being limited by the intracellular quota of P). This results in high DOC exudation by phytoplankton, which is the main source of DOC in the model. The contribution of zooplankton excretion is at a maximum in spring in the bloom region of the NW Mediterranean, but remains always much lower than that of exudation (results not shown). Similarly, the annual contribution of POC hydrolysis to the DOC production flux is weak (around 10 %). Bacteria are the first consumers of DOC, and the second ingredient for DOC accumulation is therefore a strong nutrient limitation that will highly restrict the bacteria growth rate (see Eq. 1). In this situation, DOC availability may exceed bacteria needs and result in DOC accumulation when DOC production by phytoplankton exceeds DOC uptake by bacteria. This process is enhanced in hydrodynamic situations where the surface layers are isolated from the deep waters (i.e. stratification period). Such a mechanism of DOC accumulation due to a malfunctioning microbial loop has already been described in Thingstad et al. (1997) and is also the main driver of DOC accumulation in the model. Destratification in autumn leads to a net export as well as an increase of DOC consumption through bacterial activity, driven by nutrient supply from deep water.

4.3 DOC accumulation in the light of intracellular quotas

The regions of highest DOC export fluxes correspond to the regions where the highest DOC accumulation occurs. It is therefore informative to analyze the occurrence of DOC accumulation in the light of intracellular quotas. Geographical and hydrological considerations are indeed not sufficient for a full understanding of the DOC accumulation pattern at the scale of the Mediterranean Sea.

It has already been said that, according to the model, phytoplankton exudation is the primary source of DOC. High DOC exudation by phytoplankton occurs in nutrient-depleted waters. In such a situation N and/or P phytoplankton nutrient quotas are low and limit growth rate (i.e. the cell division rate). In the model, phytoplankton (and bacteria) cell division rate is indeed controlled by the most strongly limiting element among C, N and P (see Eq. 1). In other words, the intracellular quota which is the closest to its minimum value controls the division rate. When P (and/or N) are the most strongly limiting, growth will proceed at low rate and the carbon input due to photosynthesis will rapidly meet phytoplankton needs, thus resulting in an increase in the carbon quota Q_C . Since DOC exudation flux per cell increases with Q_C through a Geider et al. (1998) non-linear quota function, DOC exudation flux will highly increase as the quota approaches its maximum value Q_C^{\max} . Phytoplankton carbon quota is therefore a good indicator of DOC exudation.

In the oligotrophic Mediterranean Sea, nutrient (and mostly P in the model) depletion is at a maximum at the end or just after the spring bloom, or under well established conditions of water stratification, thus leading to maximum exudation fluxes (see Fig. 13 and 14). In the rest of the Mediterranean, DOC exudation is at a maximum in (late) spring and summer, and mainly due to small phytoplankton. The latter is indeed characterized by low phosphorous quotas (see Fig. 10) and high carbon quotas (see Fig. 10).

The driving processes of DOC accumulation are not the same in the western and the eastern Mediterranean. In the western Mediterranean, and especially in the enlarged bloom region, large phytoplankton blooms first and is rapidly P-limited (as early as February) and the same occurs for small phytoplankton though later (i.e. only in spring, see Fig. 10). This is consistent with observations performed in the NW Mediterranean Sea (Gulf of Lions) (Diaz et al., 2001). In this situation, the high phytoplankton exudation fluxes are not only due to phytoplankton carbon quotas that are relatively high (around 50-60%, see the small phytoplankton carbon quota in Fig. 9), resulting in relatively high exudation flux per cell, but to the high phytoplankton abundance. Though exudation fluxes are high in (late) winter due to large phytoplankton (Fig. 13a), the high bacteria P-quotas (Fig. 12a) combined with winter mixing prevents DOC accumulation (Fig. 3a). In spring, and mostly in late spring, bacteria are strongly P-limited (Fig. 12b) since the bloom has rapidly consumed the available nutrients and vertical mixing has stopped. As a result, DOC accumulation starts in this region (Fig. 3b) and reaches its maximum in summer (Fig. 3c) during the stratification period since DOC exudation by phytoplankton still proceeds (though at a lower rate) and bacteria are still strongly P-limited (Fig. 12c). Finally, the end of the stratification in autumn will not only dilute the DOC-rich surface concentrations with DOC-poor deep waters, but allow the P-enrichment of surface waters (see the increase in bacteria Q_P in Fig. 12d).

In the eastern Mediterranean, DOC accumulation is mainly visible along the southern and eastern coasts. Moreover, it starts later than in the western Mediterranean (i.e. in summer against spring for the west), and is at a maximum in autumn. In the model, the Atlantic waters that flow along the coast are less dense (with densities slightly underestimated as compared to in situ measurements (Beuvier, 2011)) and therefore strongly isolated from the rest of the water column. As a result, their nutrient content will be progressively consumed and these waters become more and more oligotrophic as they flow along the southern coast of the basin, and always remain more oligotrophic than the rest of the eastern basin. In summer and autumn, they can even be considered as ultra-oligotrophic (see the phytoplankton Q_P in Fig. 10c and d). Moreover, they extend over a layer of around 100 m in thickness in which concentrations are roughly homogeneous. During summer and autumn, bacteria are also strongly P-limited but more and more carbon-rich (see Fig. 11) since phytoplankton exudation still proceeds (though at extremely low rates in autumn). Moreover, the vertical mixing that starts in autumn is not sufficiently deep to reach the nutrient-rich waters since the MLD is shallower than the bottom of these Atlantic waters. In addition, since DOC concentration is high over the

585 whole layer, DOC surface concentrations are not diluted by the mixing. As a result, accumulation
still proceeds until winter during which higher MLD will allow the P-enrichment in surface waters
and dilute surface DOC concentrations as well.

Furthermore, DOC concentrations (as well as DOC annual export flux though this is more difficult
to see in Fig.5) are negligible throughout the year in some well-identified regions, namely the two
590 cyclonic structures in the Tyrrhenian Sea, the south of the Adriatic Sea (excluding the coastal zones),
and the region of the Rhodes Gyre in the Levantine basin. All these structures are characterized by
regular input of nutrients from deep waters, resulting in an absence of strong P-limitation in bacteria.
Under such conditions, the bacteria carbon quota is rather low and DOC accumulation and export
cannot occur.

595 Finally, the strong link between low phosphate availability in the upper surface water of the
Mediterranean Sea and DOC accumulation due to nutrient limitation of bacterial production that is
evidenced in this modeling study is consistent with previous in situ (Moutin et al., 2002; Van Wambeke
et al., 2002) and modeling (Thingstad et al., 1997) studies and is shown to apply at the scale of the
whole of the Mediterranean Sea, with the exception of the aforementioned specific regions.

600 **4.4 Robustness of results**

Though difficult to achieve in a rigorous way, the robustness of our main results will be discussed in
the following section. As shown in section (2.2), the model includes many DOC and POC produc-
tion and consumption processes. A sensitivity study on all the parameters they involve is obviously
impossible to achieve, though some steps towards this goal have already been made in Baklouti
605 et al. (2006b). Moreover, accounting for the fact that most of the parameters used have a physio-
logical significance (including cell size considerations), and constitute a coherent set that remains
unchanged for the different studies undertaken with Eco3M-MED (even outside the Mediterranean),
we consider that their values are reasonably reliable. However, the POC to DOC degradation (i.e.
hydrolysis) rate and the sinking velocity are not physiological parameters and their impact on the
610 results will be discussed later.

The comparison of DOC stocks with the few available results (see the Supplementary Material)
showed that, though the shape of the modeled DOC vertical profiles were quite different (but the
values were in the same order of magnitude) from those measured, modeled and measured integrated
DOC stocks over the 0-100 m layer showed much better agreement. Furthermore, when compared
615 to in situ estimations of DOC export from the DyFaMed station (Avril, 2002) and the Adriatic and
Tyrrhenian seas (Santinelli et al., 2013), the model always provides higher DOC export values. These
differences in DOC export may be partly attributable to the model failures discussed the Supplemen-
tary Material but, as already mentioned, in situ estimations also involve considerable uncertainties.
Hence, according to Santinelli et al. (2013), DOC export computations from stock differences below
620 the euphotic layer probably underestimate the real flux. This is also the conclusion we came to by

using model outputs to compute export fluxes with our method and with the in situ method. If we assume, however, that the different in situ estimations are consistent with each other, it appears that the highest DOC export occurs in the Adriatic Sea, followed by the DyFaMed station (Ligurian Sea) and then by the Tyrrhenian Sea, and the same order can be inferred from the model outputs.

625 Two parameters are essential in POC export, namely POC to DOC degradation rate and the sinking velocity.

Since our model includes a single detrital compartment, an intermediate value of 2 m d^{-1} has been used for the sinking velocity. This value is intended to be representative of the high sinking rates ($> 100 \text{ m/day}$) of very large particles as well as the very low sinking rates of small particles. 630 It may however reflect an underestimation of the actual mean value though this is difficult to verify. In several other models (e.g. Lévy et al., 1998; Lacroix and Gregoire, 2002; Herrmann and Somot, 2008), two detrital compartments are used, thus making it possible to differentiate between low and high sinking rates of detrital particles. However, in these models, the large detrital compartment (to which high sinking rates are affected) is only fueled by zooplankton fecal pellets (Lévy et al., 1998; 635 Herrmann and Somot, 2008) and by mesozooplankton mortality in Lacroix and Gregoire (2002). These fluxes, except the latter, are probably weak compared to the other POC sources in our model (which is dominated by the mortality of the largest organisms). Finally, in these models, the remaining sources of POC fuel the small detrital compartment for which the sinking velocities are lower than that used in our model. To conclude on this point, adding complexity in a given model generally 640 leads to the multiplication of the number of state variables and parameters. When these parameters and/or these new processes are not well known, this also adds uncertainty, and in this case complexity does not necessarily lead to a better agreement between model outputs and observations as this is suggested by several studies (e.g. Muller et al., 2009; Kriest et al., 2010; Paudel and Jawitz, 2012). With the addition of a class of large detrital particles, the sinking velocity associated with this 645 detrital compartment as well as the definition of the processes that would have fueled this additional compartment (the latter are not the same in the different aforementioned models that use two detrital compartments) would have added a source of uncertainty in the model. As a consequence, the particulate carbon fluxes wouldn't necessarily have been more realistic than the ones provided by this study. The same conclusion may apply as regards the aggregation models which formulations are 650 generally empirical and associated with parameters that are hardly measurable.

More importantly, it can be considered that the likely underestimated sinking velocity used in the present model is compensated by the very low POC degradation rate. In our model, its maximum value is set at 0.03 d^{-1} but it is modulated by the bacteria carbon quota. In substance, the higher the carbon quota, the more the degradation rate decreases and eventually becomes 0 when the bacteria 655 carbon quota is maximum. As a result, the effective POC degradation rate is always less than 0.03 d^{-1} in the model, and it is lower in the surface layers since bacteria are more rich in carbon than in deep waters. It is also lower than all the values used in the aforementioned models. Concerning

in situ data for the degradation rate, Sempéré et al. (2000) have determined values at 50 and 200 m for labile and less labile POC in three regions of the Mediterranean Sea, showing that, for the labile POC (which represent a significant part in the latter study), the degradation rate can be up to 100 times higher than that used in the present study.

Apart from these two parameters, it has been seen that the model underestimates Chl concentrations at the DCM (mainly due to a lack of large phytoplankton) and this may also lead to an underestimation of POC export. However, the 0-100 m mIPP values are consistent with oIPP thereby suggesting that this DCM underestimation has only a limited impact on carbon production. Overall, the annual POC export flux at 100 m provided by the model is around 8% of the annual primary production, a value that is consistent with in situ estimations (Miquel et al., 1994).

Between 100 m and 200 m, however, the mean bacteria carbon quota is lower since POC hydrolysis and bacteria and heterotrophic nanoflagellate mortalities are the only sources of DOC, resulting in higher hydrolysis rates and in lower POC export at 200 m. Looking at the vertical attenuation of POC fluxes, it is common to use a power law expressed as $F(z) = F(z = z_0) * (\frac{z}{z_0})^{-b}$, where $F(z)$ is the depth-dependent POC flux and b a positive coefficient whose values may vary according to the location or the period. In regions of significant export, b values inferred from the model outputs fluctuate between 0.9 in the Provencal sub-basin and 2.3 for the Algerian basin. Values of b derived from observations tend to be lower, i.e. respectively equal to 0.92 and 1.0 for the western and eastern moorings (Gogou et al., 2014), or 0.75 in the Alboran Sea (Zúñiga et al., 2007). This again suggests that the attenuation of POC export flux between 100 m and 200 m is too great in the model. Furthermore, when compared to the few available data for POC export fluxes, the model always underestimates the export flux in the eastern basin. However, all the in situ estimations we could find in the literature were done at 150 m or 200 m depth, which means in the 100-200 m layer where the modeled POC export is more likely to be underestimated. In summary, all this suggests that the underestimation of POC export fluxes is more to be the case at 200 m than at 100 m depth though the comparison at the DyFaMed station shows that the mean mPOC export rate ($5.6 \text{ gC.m}^{-2}.\text{y}^{-1}$ and $2.2 \text{ gC.m}^{-2}.\text{y}^{-1}$ at 100 m and 200 m respectively) is within the range of the measured rate at 200 m (i.e. $[1.6;2.6] \text{ gC.m}^{-2}.\text{y}^{-1}$ (Copin-Montégut and Avril, 1993; Miquel et al., 2011)). Finally, it is very unlikely that these uncertainties could shed doubt on the predominance of DOC in the OC export in the eastern basin. This conclusion also applies in the western basin (though with less certainty), all the more so in that in situ measurements allow the same conclusion to be drawn in the sampled stations of the NW Mediterranean (Copin-Montégut and Avril, 1993; Avril, 2002; Miquel et al., 2011).

5 Conclusions

A 14-year simulation combining a high resolution physical model (NEMO-MED12) and a mechanistic biogeochemical model (Eco3M-MED) has been developed to study carbon organic production and fate at the scale of the Mediterranean Sea.

695 A preliminary work presented in the Supplementary Material focused on the Model Skill Assessment through an extensive comparison of different model outputs (i.e. chlorophyll, nutrients, primary production and DOC profiles) with available data at various time and space scales. This work allowed to verify the model's ability to represent the main features of the biogeochemical functioning of the Mediterranean Sea. In the Results section, carbon export fluxes are investigated. Previous estimations
700 of DOC export in the Mediterranean Sea were restricted to specific regions of the Mediterranean (e.g. the Ligurian, Adriatic, Tyrrhenian Seas). We here propose the first Mediterranean-scale view of annual DOC and POC export fluxes, as well as an analysis of their spatial and seasonal variations in the light of plankton intracellular quotas.

The two major results of this modeling study lie in (i) the predominance of the eastern basin in
705 OC export (with nearly 60 % of the OC export occurring in the eastern basin), and (ii) in the crucial role of the dissolved fraction in the total organic carbon export. At Mediterranean scale, DOC export represents about four fifths of total organic carbon fluxes, thereby attesting to its major role in the carbon cycle and the biological pump in the Mediterranean Sea. The concept of a malfunctioning microbial loop (Thingstad et al., 1997), due to high P-limitation of both phytoplankton and bacteria
710 leading to high DOC exudation fluxes beyond bacterial needs, also applies in the present study though it is generalized to the whole of the Mediterranean Basin, except for some specific P-rich regions (see Results and Discussion). Export in the eastern basin is markedly high despite its lower productivity compared to the western basin. By contrast, POC export is closely associated with regions characterized by high productivity. As a consequence, total carbon export in the eastern
715 basin is considerably higher than expected as regards its low primary productivity. Results also show high spatial variability in organic carbon fluxes and a temporal uncoupling between POC and DOC exports. This is attributable to the differences in the processes involved in the production and export of POC and DOC.

Further comparisons with observations are clearly necessary to confirm these results, which emphasizes the need for in situ temporal monitoring to properly quantify organic carbon export. This
720 study also highlights the need to examine the microbial food web in detail in order to further investigate the carbon cycle in the Mediterranean Sea. Furthermore, the implementation of an explicit inorganic carbon compartment in the biogeochemical model would close the carbon budget and help in the full characterization of the biological pump.

725 In conclusion, the strong link between low phosphate availability in the upper surface water of the Mediterranean Sea and DOC accumulation due to nutrient limitation of bacterial production already identified by previous modeling (Thingstad et al., 1997) and in situ (Moutin et al., 2002;

Van Wambeke et al., 2002) studies, is confirmed by this modeling study, which may therefore be of interest for other oceanic regions. The low phosphate availability of the upper waters has been identified in other oceanic regions such as the Sargasso Sea (Wu et al., 2000), the North Pacific and the South West Pacific (Van Den Broeck et al., 2004), and high DOC accumulation has also been reported in some of these areas (Carlson et al., 1994). This work may therefore be of interest for these oceanic regions. Finally, in the context of climate change, the enhanced stratification and the probable geographical extension of low phosphate availability in upper waters (Karl et al., 1997; Moutin et al., 2008) is expected to result in an increase in DOC production (Santinelli et al., 2013; Lazzari et al., 2013), and thereby further increase the importance of DOC in the biological carbon pump.

Acknowledgements. The authors are grateful to the various organisations that funded this work. This includes the French PACA Region (which funded the PhD thesis of A. Guyennon), the Mercator Ocean group (which funded the SiMED project that provided an efficient framework for this work), the MED-ICCBIO project (funded by the *Groupement d' Intérêt Scientifique* "Climat, Environnement et Société"), and the OT-MED Labex. This work is a contribution to the Labex OT-Med (n° ANR-11-LABEX-0061) funded by the French Government "Investissements d'Avenir" program of the French National Research Agency (ANR) through the A*MIDEX project (n° ANR-11-IDEX-0001-02). It is also a contribution to the MerMEX-MISTRALS program and it was granted access to the HPC resources of IDRIS (Institut du Développement et des Ressources en Informatique Scientifique) of the Centre National de la Recherche Scientifique (CNRS). The DYFAMED time series was provided by the Oceanological Observatory (CNRS-UPMC) of Villefranche-sur-Mer (L.Coppola). This project is funded by CNRS-INSU and ALLENI through the MOOSE observation network. The satellite data used in this study are MyOcean Products. Authors are also grateful to Jean-Michel André for his help and valuable advice, and to L. Coppola for his very efficient assistance in obtaining in situ data from the DyFaMed station and to Antoine Mangin (Société ACRI - Sophia-Antipolis, France).

References

- Alekseenko, E., Raybaud, V., Espinasse, B., Carlotti, F., Queguiner, B., Thouvenin, B., Garreau, P., and Baklouti, M.: Seasonal dynamics and stoichiometry of the planktonic community in the NW Mediterranean Sea: a 3D modeling approach, *Ocean Dynamics*, 64, 179–207, 2014.
- 755
- Avril, B.: DOC dynamics in the northwestern Mediterranean Sea (DYFAMED site), *Deep Sea Research Part II: Topical Studies in Oceanography*, 49, 2163–2182, 2002.
- Baklouti, M., Diaz, F., Pinazo, C., Faure, V., and Quéguiner, B.: Investigation of mechanistic formulations depicting phytoplankton dynamics for models of marine pelagic ecosystems and description of a new model, *Progress in Oceanography*, 71, 1–33, 2006a.
- 760
- Baklouti, M., Faure, V., Pawlowski, L., and Sciandra, A.: Investigation and sensitivity analysis of a mechanistic phytoplankton model implemented in a new modular numerical tool (Eco3M) dedicated to biogeochemical modelling, *Progress in Oceanography*, 71(1), 34–58, 2006b.
- Baklouti, M., Chevalier, C., Bouvy, M., Corbin, D., Pagano, M., Troussellier, M., and Arfi, R.: A study of plankton dynamics under osmotic stress in the Senegal River Estuary, West Africa, using a 3D mechanistic model, *Ecological Modelling*, 222, 2704–2721, 2011.
- 765
- Baretta, J., Ebenhoh, W., and Ruardij, P.: The European Regional Seas Ecosystem Model, a complex marine ecosystem model, *J. Sea Res.*, 33, 233–246, 1995.
- Béranger, K., Mortier, L., and Crépon, M.: Seasonal variability of water transport through the Straits of Gibraltar, Sicily and Corsica, derived from a high-resolution model of the Mediterranean circulation, *Progress in Oceanography*, 66, 341–364, 2005.
- 770
- Bertilsson, S., Berglund, O., Karl, D. M., and Chisholm, S. W.: Elemental composition of marine *Prochlorococcus* and *Synechococcus*: Implications for the ecological stoichiometry of the sea, *Limnol. Oceanogr.*, 48, 1721–1731, 2003.
- 775
- Beuvier, J.: Modélisation de la variabilité climatique de la circulation et des masses d’eau en mer Méditerranée: impact des échanges océan-atmosphère, Ph.D. thesis, Ecole Polytechnique, 2011.
- Beuvier, J., Sevault, F., Herrmann, M., Kontoyiannis, H., Ludwig, W., Rixen, M., Stanev, E., Béranger, K., and Somot, S.: Modeling the Mediterranean Sea interannual variability during 1961–2000: focus on the Eastern Mediterranean Transient, *Journal of Geophysical Research: Oceans* (1978–2012), 115, doi:10.1029/2009JC005950, 2010.
- 780
- Beuvier, J., Béranger, K., Brossier, C., Somot, S., Sevault, F., Drillet, Y., Bourdallé-Badief, R., Ferry, N., Lyard, F., et al.: Spreading of the Western Mediterranean Deep Water after winter 2005: Time scales and deep cyclone transport., *Journal of Geophysical Research*, 117, doi:10.1029/2011JC007679, 2012a.
- Beuvier, J., Lebeaupin Brossier, C., Béranger, K., Arsouze, T., Bourdallé-Badie, R., C., D., Drillet, Y., Drobin-ski, P., Lyard, F., Ferry, N., Sevault, F., and Somot, S.: Oceanic component for the modeling of the regional Mediterranean Earth System., *Mercator Ocean Quarterly Newsletter*, 46, 60–66, 2012b.
- 785
- Boldrin, A., Misericocchi, S., Rabitti, S., Turchetto, M., Balboni, V., and Socal, G.: Particulate matter in the southern Adriatic and Ionian Sea: characterisation and downward fluxes, *Journal of Marine Systems*, 33, 389–410, 2002.
- 790
- Bopp, L., Monfray, P., Aumont, O., Dufresne, J., Le Treut, H., Madec, G., Terray, L., and Orr, J.: Potential climate change on marine export production, *Global Biogeochemical Cycles*, 15, 81–99, 2001.

- Bosc, E., Bricaud, A., and Antoine, D.: Seasonal and interannual variability in algal biomass and primary production in the Mediterranean Sea, as derived from 4 years of SeaWiFS observations, *Global Biogeochemical Cycles*, 18, GB1005, doi:10.1029/2003GB002034, 2004.
- 795 Brown, E. J. and Harris, R. F.: Kinetics of algal transient phosphate uptake and the cell quota concept, *Limnol. Oceanogr.*, 23, 35–40, 1978.
- Buesseler, K.: Do upper-ocean sediment traps provide an accurate record of particle flux ?, *Nature*, 353, 420–423, 1991.
- Carlson, C., Ducklow, H., and Michaels, A.: Annual flux of dissolved organic carbon from the euphotic zone in
800 the northwestern Sargasso Sea, *Nature*, 371, 405–408, 1994.
- Christaki, U., Courties, C., Joux, F., Jeffrey, W. H., Neveux, J., and Naudin, J.: Community structure and trophic role of ciliates and heterotrophic nanoflagellates in Rhone River diluted mesoscale structures (NW Mediterranean Sea), *Aquat Microb Ecol*, 57, 263–277, 2009.
- Claustre, H., Morel, A., Hooker, S., Babin, M., Antoine, D., Oubelkheir, K., Bricaud, A., Leblanc, K.,
805 Queguiner, B., and Maritorena, S.: Is desert dust making oligotrophic waters greener ?, *Geophysical Research Letters*, 29, 107–1–107–4, 2002.
- Copin-Montégut, G. and Avril, B.: Vertical distribution and temporal variation of dissolved organic carbon in the North-Western Mediterranean Sea, *Deep Sea Research Part I: Oceanographic Research Papers*, 40, 1963–1972, 1993.
- 810 Crise, A., Crispi, G., and Mauri, E.: A seasonal three-dimensional study of the nitrogen cycle in the Mediterranean Sea: Part I. Model implementation and numerical results, *Journal of Marine Systems*, 18, 287–312, 1998.
- Crispi, G., Crise, A., and Solidoro, C.: Three-dimensional oligotrophic ecosystem models driven by physical forcing: the Mediterranean Sea case, *Environmental Modelling Software*, 13, 483–490, 1998.
- 815 Diaz, F., Raimbault, P., Boudjellal, B., Garcia, N., and Moutin, T.: Early spring phosphorus limitation of primary productivity in a NW Mediterranean coastal zone (Gulf of Lions), *Marine Ecology Progress Series*, 211, 51–62, 2001.
- D’Ortenzio, F., Marullo, S., Ragni, M., Ribera d’Alcalà, M., and Santoleri, R.: Validation of empirical SeaWiFS algorithms for chlorophyll-a retrieval in the Mediterranean Sea: A case study for oligotrophic seas, *Remote
820 Sensing of Environment*, 82, 79–94, 2002.
- Droop, M.: Vitamin B12 and marine ecology. IV. The kinetics of uptake, growth and inhibition in *Monochrysis lutheri*, *J. Mar. Biol. Assoc. UK*, 48, 689–733, 1968.
- Droop, M.: The nutrient status of algal cells in batch culture, *J. Mar. Biol. Assoc. UK*, 55, 541–555, 1975.
- Eppley, R. and Peterson, B.: Particulate organic matter flux and planktonic new production in the deep ocean,
825 *Nature*, 282, 677–680, 1979.
- Fasham, M., Flynn, K., Pondaven, P., Anderson, T., and Boyd, P.: Development of a robust marine ecosystem model to predict the role of iron in biogeochemical cycles: A comparison of results for iron-replete and iron-limited areas, and the SOIREE iron-enrichment experiment, *Deep Sea Research Part I: Oceanographic Research Papers*, 53, 333–366, 2006.
- 830 Fukuda, R., Ogawa, H., Nagata, T., and Koike, I.: Direct Determination of Carbon and Nitrogen Contents of Natural Bacterial Assemblages in Marine Environments, *Appl Environ Microbiol*, 64, 3352–3358, 1998.

- Garcia, H. E., Locarnini, R., Boyer, T., and Antonov, J.: World Ocean Atlas 2005. Vol. 4, Nutrients (phosphate, nitrate, silicate), 2006.
- Geider, R., MacIntyre, H., and Kana, T.: A dynamic regulatory model of phytoplankton acclimation to light, nutrients, and temperature, *Limnology and Oceanography*, 43, 679–694, 1998.
- 835 Gogou, A., Sanchez-Vidal, A., Durrieu de Madron, X., Stavrakakis, S., Calafat, A. M., Stabholz, M., Psarra, S., Canals, M., Heussner, S., Stavrakaki, I., et al.: Carbon flux to the deep in three open sites of the Southern European Seas (SES), *Journal of Marine Systems*, 129, 224–233, 2014.
- Gómez, F.: The role of the exchanges through the Strait of Gibraltar on the budget of elements in the Western Mediterranean Sea: consequences of human-induced modifications, *Marine Pollution Bulletin*, 46, 685–694, 840 2003.
- Hansell, D. and Carlson, C.: Marine Dissolved Organic Matter and the Carbon Cycle, *Oceanography*, 14, 685–716, 2001.
- Hansell, D., Carlson, C., and Suzuki, Y.: Dissolved organic carbon export with North Pacific Intermediate Water formation, *Global Biogeochemical Cycles*, 16, 7–1–7–8, 2002.
- 845 Hansell, D., Repeta, D., Carlson, C., and Schlitzer, R.: Dissolved organic matter in the ocean: A controversy stimulates new insights, *Oceanography*, 22, 202–211, 2009.
- Heldal, M., Scanlan, D. J., Norland, S., Thingstad, F., and Mann, N. H.: Elemental composition of single cells of various strains of marine *Prochlorococcus* and *Synechococcus* using X-ray microanalysis, *Limnol. Oceanogr.*, 48, 1732–1743, 2003.
- 850 Herrmann, M. and Somot, S.: Relevance of ERA40 dynamical downscaling for modeling deep convection in the Mediterranean Sea, *Geophysical Research Letters*, 35, doi:10.1029/2007GL032442, 2008.
- Herrmann, M., Diaz, F., Estournel, C., Marsaleix, P., and Ulses, C.: Impact of atmospheric and oceanic interannual variability on the Northwestern Mediterranean Sea pelagic planktonic ecosystem and associated carbon cycle, *Journal of Geophysical Research: Oceans*, 118, 1–22, 2014.
- 855 Holling, C.: Some characteristics of simple types of predation and parasitism, *The Canadian Entomologist*, 91, 385–398, 1959.
- Karl, D. M., Letelier, R. M., Tupas, L., Dore, J., Christian, J., and Hebel, D.: The role of nitrogen fixation in biogeochemical cycling in the subtropical North Pacific Ocean, *Nature*, 387, 533–538, 1997.
- 860 Klausmeier, C., Litchman, E., and Levin, S.: Phytoplankton growth and stoichiometry under multiple nutrient limitation, *Limnology and Oceanography*, 49, 1463–1470, 2004.
- Klausmeier, C., Litchman, E., Daufresne, T., and Levin, S.: Phytoplankton stoichiometry, *Ecol. Res.*, 23, 479–485, 2008.
- Kooijman, S. A. L. M.: *Dynamic Energy and Mass Budgets in Biological Systems*, Cambridge University Press, 865 Cambridge, UK, 2000.
- Kriest, I., Khatiwala, S., and Oeschlies, A.: Towards an assessment of simple global marine biogeochemical models of different complexity, *Progress in Oceanography*, 86, 337–360, 2010.
- Lacroix, G. and Gregoire, M.: Revisited ecosystem model (MODECOGeL) of the Ligurian Sea: seasonal and interannual variability due to atmospheric forcing, *Journal of Marine Systems*, 37, 229–258, 2002.

- 870 Lazzari, P., Mattia, G., Solidoro, C., Salon, S., Crise, A., Zavatarelli, M., Oddo, P., and Vichi, M.: The impacts of climate change and environmental management policies on the trophic regimes in the Mediterranean Sea: Scenario analyses, *Journal of Marine Systems*, 2013.
- Le Quéré, C., Takahashi, T., Buitenhuis, E., Rödenbeck, C., and Sutherland, S.: Impact of climate change and variability on the global oceanic sink of CO₂, *Global Biogeochemical Cycles*, 24, 2016–2040, 2010.
- 875 Le Quéré, C. L., Harrison, S., P., C., Buitenhuis, E., Aumont, O., Bopp, L., Claustre, H., Cotrim Da Cunha, L., Geider, R., Giraud, X., et al.: Ecosystem dynamics based on plankton functional types for global ocean biogeochemistry models, *Global Change Biology*, 11, 2016–2040, 2005.
- Leblanc, K., Quéguiner, B., Garcia, N., Rimmelin, P., and Raimbault, P.: Silicon cycle in the NW Mediterranean Sea: seasonal study of a coastal oligotrophic site, *Oceanologica Acta*, 26, 339–355, 2003.
- 880 Lefèvre, D., Denis, M., Lambert, C., and Miquel, J.: Is DOC the main source of organic matter remineralization in the ocean water column ?, *Journal of Marine Systems*, 7, 281–291, 1996.
- Lévy, M., Mémerly, L., and André, J.: Simulation of primary production and export fluxes in the Northwestern Mediterranean Sea, *Journal of Marine Research*, 56, 197–238, 1998.
- Lovdal, T., Skjoldal, E. F., Heldal, M., Norland, S., and Thingstad, T. F.: Changes in morphology and elemental composition of *Vibrio splendidus* along a gradient from carbon-limited to phosphate-limited growth, *Microb. Ecol.*, 55, 152–161, 2008.
- 885 Ludwig, W.: Continental erosion and river transport of organic carbon to the world's Oceans, Ph.D. thesis, Université Louis Pasteur de Strasbourg, 1996.
- Ludwig, W., Dumont, E., Meybeck, M., and Heussner, S.: River discharges of water and nutrients to the Mediterranean and Black Sea: Major drivers for ecosystem changes during past and future decades?, *Progress in Oceanography*, 80, 199–217, 2009.
- 890 Macías, D., Stips, A., and Garcia-Gorriz, E.: The relevance of deep chlorophyll maximum in the open Mediterranean Sea evaluated through 3D hydrodynamic-biogeochemical coupled simulations, *Ecological Modelling*, 281, 26–37, 2014.
- 895 Madec, G. and The-NEMO-Team: NEMO ocean engine, Note du pole de modélisation de l'IPSL, 27, 1228–1619, 2008.
- Maier-Reimer, E., Mikolajewicz, U., and Winguth, A.: Future ocean uptake of CO₂: interaction between ocean circulation and biology, *Climate Dynamics*, 12, 711–722, 1996.
- Marshall, J. and Schott, F.: Open-ocean convection: Observations, theory, and models, *Reviews of Geophysics*, 900 37, 1–64, 1999.
- Marty, J. and Chiavérini, J.: Hydrological changes in the Ligurian Sea (NW Mediterranean, DYFAMED site) during 1995–2007 and biogeochemical consequences, *Biogeosciences*, 7, 2117–2128, 2010.
- Marty, J.-C., Garcia, N., and Raimbault, P.: Phytoplankton dynamics and primary production under late summer conditions in the NW Mediterranean Sea, *Deep Sea Research Part I*, 55, 1131–1149, 2008.
- 905 Mattia, G., Zavatarelli, M., Vichi, M., and Oddo, P.: The Eastern Mediterranean Sea biogeochemical dynamics in the 1990s: A numerical study, *Journal of Geophysical Research: Oceans*, 118, 2231–2248, 2013.
- Mauriac, R., Moutin, T., and Baklouti, M.: Accumulation of DOC in Low Phosphate Low Chlorophyll (LPLC) area: is it related to higher production under high N: P ratio?, *Biogeosciences*, 8, 933–950, 2011.

- Meador, T., Gogou, A., Spyres, G., Herndl, G., Krasakopoulou, E., Psarra, S., Yokokawa, T., De Corte, D.,
 910 Zervakis, V., and Repeta, D.: Biogeochemical relationships between ultrafiltered dissolved organic matter
 and picoplankton activity in the Eastern Mediterranean Sea, *Deep Sea Research Part II: Topical Studies in
 Oceanography*, 57, 1460–1477, 2010.
- Millot, C. and Taupier-Letage, I.: Circulation in the Mediterranean sea, in: *The Mediterranean Sea*, pp. 29–66,
 Springer, 2005.
- 915 Miquel, J., Martín, J., Gasser, B., Rodriguez-y Baena, A., Toubal, T., and Fowler, S.: Dynamics of particle flux
 and carbon export in the northwestern Mediterranean Sea: a two decade time-series study at the DYFAMED
 site, *Progress in Oceanography*, 91, 461–481, 2011.
- Miquel, J. C., Fowler, S. W., La Rosa, J., and Buat-Menard, P.: Dynamics of the downward flux of particles and
 carbon in the open northwestern Mediterranean Sea, *Deep-Sea Research I*, 41, 243–261, 1994.
- 920 Moore, J. K., Doney, S. C., Kleypas, J. A., Glover, D. M., and Fung, I. Y.: An intermediate complexity marine
 ecosystem model for the global domain, *Deep-Sea Research II*, 49, 403–462, 2002.
- Morel, A.: Optical modeling of the upper ocean in relation to its biogenous matter content (case I waters),
Journal of Geophysical Research: Oceans (1978–2012), 93, 10 749–10 768, 1988.
- Moutin, T. and Raimbault, P.: Primary production, carbon export and nutrients availability in Western and
 925 Eastern Mediterranean Sea in early summer 1996 (MINOS cruise), *Journal of Marine Systems*, 33, 273–288,
 2002.
- Moutin, T., Thingstad, T. F., Van Wambeke, F., Marie, D., Slawyk, G., and Raimbault, P.: Does competition for
 nanomolar phosphate supply explain the predominance of the cyanobacterium *Synechococcus*?, *Limnology
 and Oceanography*, 47, 1562–1567, 2002.
- 930 Moutin, T., Karl, D. M., Duhamel, S., Rimmelin, P., Raimbault, P. and Van Mooy, B. A. S., and Claustre, H.:
 Phosphate availability and the ultimate control of new nitrogen input by nitrogen fixation in the tropical
 Pacific Ocean, *Biogeosciences*, 5, 95–109, 2008.
- Moutin, T., Van Wambeke, F., and Prieur, L.: Introduction to the Biogeochemistry from the Oligotrophic to the
 Ultraoligotrophic Mediterranean (BOUM) experiment, *Biogeosciences*, 9, 3817–3825, 2012a.
- 935 Muller, S., Muñoz-Carpena, R., and Kiker, G.: Model Relevance: Frameworks for Exploring the Complexity-
 Sensitivity-Uncertainty Trilemma, in: *Climate: Global Change and Local Adaptation*, edited by Linkov, I.
 and Bridges, T. S., Springer, Dordrecht, 2009.
- Palmiéri, J.: Modélisation biogéochimique de la mer Méditerranée avec le modèle régional couplé NEMO-
 MED12/PISCES., Ph.D. thesis, Université de Versailles Saint-Quentin, France, 2014.
- 940 Palmiéri, J., Le Vu, B., Dutay, J., Bopp, L., Béranger, K., Beuvier, J., Somot, S., and Éthé, C.: Biogeochemical
 modelling of the Mediterranean Sea with PISCES MED-12 model., *GMD*, in prep.
- Pasqueron de Fommervault, O., Migon, C., D’Ortenzio, F., Ribera d’Alcalà, M., and Coppola, L.: Temporal
 variability of nutrient concentrations in the northwestern Mediterranean sea (DYFAMED time-series station),
Deep Sea Research Part I, 100, 1–12, 2015.
- 945 Paudel, R. and Jawitz, J.: Does increased model complexity improve description of phosphorus dynamics in a
 large treatment wetland?, *Ecological Engineering*, 42, 283–294, 2012.
- Prowe, A., Pahlow, M., Dutkiewicz, S., Follows, M., and Oschlies, A.: Top-down control of marine phytoplank-
 ton diversity in a global ecosystem model, *Progress in Oceanography*, 101, 1–13, 2012.

- Redfield, A. C.: The biological control of chemical factors in the environment, *Am Sci*, 46, 205–221, 1958.
- 950 Santinelli, C., D.A., H., and d'Alcala M., R.: Influence of stratification on marine dissolved organic carbon (DOC) dynamics : The Mediterranean Sea case, *Progress in Oceanography*, 119, 68–77, 2013.
- Sarmiento, J. and Gruber, N.: *Ocean biogeochemical dynamics*, vol. 1015, Princeton University Press Princeton, 2006.
- Sarmiento, J., Hughes, T., Stouffer, R., and Manabe, S.: Simulated response of the ocean carbon cycle to anthropogenic climate warming, *Nature*, 393, 245–249, 1998.
- 955 Schaap, D. and Lowry, R.: SeaDataNet–Pan-European infrastructure for marine and ocean data management: unified access to distributed data sets, *International Journal of Digital Earth*, 3, 50–69, 2010.
- Sempéré, R., Yoro, S. C., Van Wambeke, F., and Charrière, B.: Microbial decomposition of large organic particles in the Northwestern Mediterranean Sea: an experimental approach, *Mar Ecol Prog Ser*, 198, 61–72, 960 2000.
- Siegenthaler, U. and Sarmiento, J.: Atmospheric carbon dioxide and the ocean, *Nature*, 365, 119–125, 1993.
- Siokou-Frangou, I., Christaki, U., Mazzocchi, M., Montresor, M., Ribera d'Alcalà, M., Vaqué, D., and Zingone, A.: Plankton in the open Mediterranean Sea: a review, *Biogeosciences*, 7, 1543–1586, 2010.
- Somot, S., Sevault, F., and Déqué, M.: Transient climate change scenario simulation of the Mediterranean Sea 965 for the twenty-first century using a high-resolution ocean circulation model, *Climate Dynamics*, 27, 851–879, 2006.
- Talarmin, A., Van Wambeke, F., Duhamel, Catala, P., Moutin, T., and Lebaron, P.: Improved methodology to measure taxon-specific phosphate uptake in live and unfiltered samples, *Limnol. Oceanogr. Methods*, 9, 443–453, doi:10.4319/lom.2011.9.443., 2011.
- 970 Thingstad, T., Hagström, A., and Rassoulzadegan, F.: Accumulation of degradable DOC in surface waters: Is it caused by a malfunctioning microbial loop?, *Limnology and Oceanography*, 42, 398–404, 1997.
- Thingstad, T., Krom, M., Mantoura, R., Flaten, G., Groom, S., Herut, B., Kress, N., Law, C., Pasternak, A., Pitta, P., Psarra, S., Rassoulzadegan, F., Tanaka, T., Tselepidis, A., Wassman, P., Woodward, E., Wexels, R., Zodiatis, G., and Zohary, T.: Nature of phosphorus limitation in the ultraoligotrophic eastern Mediterranean, 975 *Science*, 309, 1068–1071, 2005.
- Toggweiler, J., Gnanadesikan, A., Carson, S., Murnane, R., and Sarmiento, J.: Representation of the carbon cycle in box models and GCMs: 1. Solubility pump, *Global biogeochemical cycles*, 17, 2003.
- Tugrul, S. and Besiktepe, S.: Nutrient exchange fluxes between the black sea and the Mediterranean through the turkish strait system (marmara sea, bosphorus and dardanelles), *CIESM*, 2007.
- 980 Vallina, S., Ward, B., Dutkiewicz, S., and Follows, M.: Maximal feeding with active prey-switching: A kill-the-winner functional response and its effect on global diversity and biogeography, *Progress in Oceanography*, 120, 93–109, 2014.
- Van Den Broeck, N., Moutin, T., Rodier, M., and Le Bouteiller, A.: Seasonal variations of phosphate availability in the SW Pacific Ocean near New Caledonia, *Mar. Ecol. Progress Ser.*, 268, 1–12, 2004.
- 985 Van Wambeke, F., Christaki, U., Giannakourou, A., Moutin, T., and Souvemerzoglou, K.: Longitudinal and vertical trends of bacterial limitation by phosphorus and carbon in the Mediterranean Sea, *Microbial ecology*, 43, 119–133, 2002.

- Vichi, M., Pinardi, N., and Masina, S.: A generalized model of pelagic biogeochemistry for the global ocean ecosystem. Part I: Theory, *Journal of Marine Systems*, 64, 89–109, 2007.
- 990 Volpe, G., Santoleri, R., Vellucci, V., Ribera d'Alcala, M., Marullo, S., and d'Ortenzio, F.: The colour of the Mediterranean Sea: Global versus regional bio-optical algorithms evaluation and implication for satellite chlorophyll estimates, *Remote Sensing of Environment*, 107, 625–638, 2007.
- Vörösmarty, C., Fekete, B., and Tucker, B.: Global river discharge database, RivDis, Tech. rep., 1996.
- Wilhelm, S. W., King, A. L., Twining, B. S., LeClerc, G. R., DeBruyn, J. M., Strzepek, R. F., Breene, C. L.,
995 Pickmere, S., Ellwood, M. J., Boyd, P. W., and Hutchins, D. A.: Elemental quotas and physiology of a south-western Pacific Ocean plankton community as a function of iron availability, *Aquatic Microbial Ecology*, 68, 185–194, 2013.
- Wu, J., SUNDA, W., BOYLE, E., and Karl, D.: Phosphate depletion in the western North Atlantic Ocean, *Sciences*, 289, 759–762, 2000.
- 1000 Zúñiga, D., Calafat, A., Sanchez-Vidal, A., Canals, M., Price, B., Heussner, S., and Miserocchi, S.: Particulate organic carbon budget in the open Algero-Balearic Basin (Western Mediterranean): Assessment from a one-year sediment trap experiment, *Deep Sea Research Part I: Oceanographic Research Papers*, 54, 1530–1548, 2007.

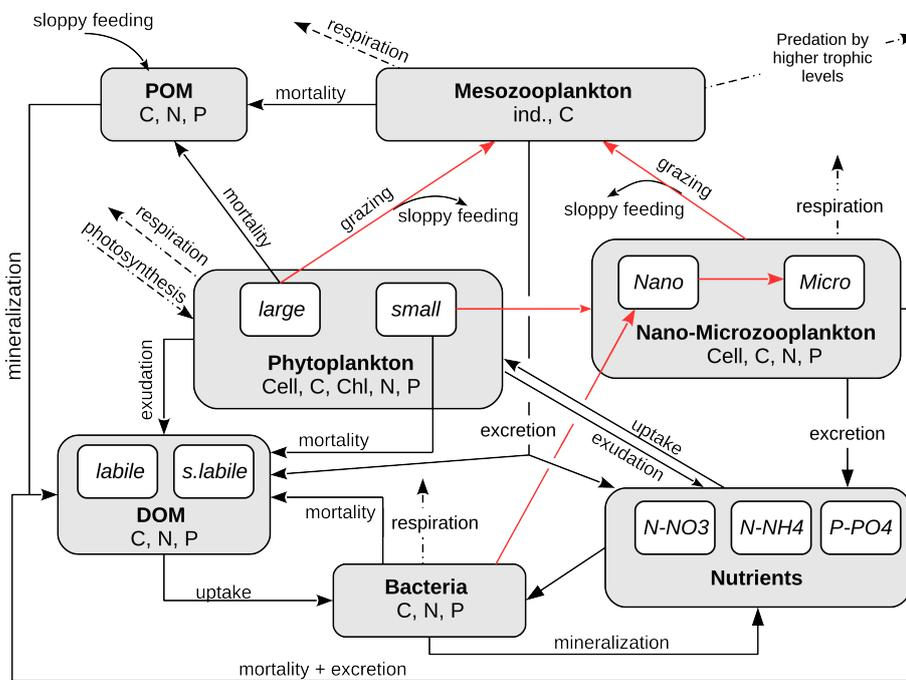


Figure 1. Conceptual diagram of the biogeochemical model Eco3M-MED. Grey boxes represent major compartments and white boxes sub-compartments. State variables for each sub-compartment are listed at the bottom of compartment boxes. Red arrows indicate grazing processes from the prey to the predator.

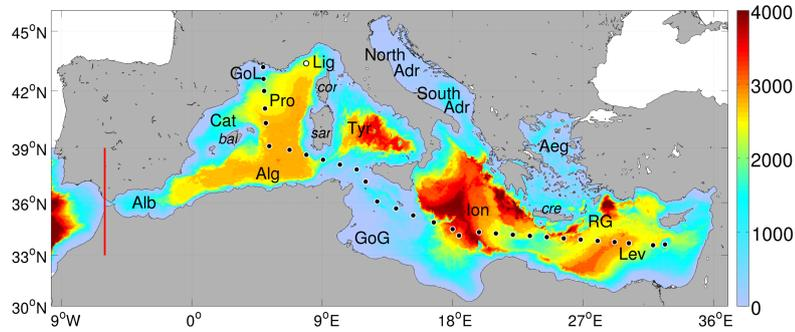


Figure 2. Bathymetry of the grid in meters, black dots represent the BOUM cruise stations (Moutin et al., 2012a) while white dot is DyFaMed position (Marty and Chiavérini, 2010). The area west of the red line constitutes the buffer-zone. Acronyms indicate different sub-basin names and islands (in italic). Terminology is taken from Millot and Taupier-Letage (2005). From west to east, **Alb** stands for Alboran Sea, **Cat** for Catalan Sea, **GoL** for Gulf of Lions, **Pro** for Provençal sub-basin, **Alg** for Algerian basin, **Lig** for Ligurian Sea, **Tyr** for Tyrrhenian Sea, **GoG** for Gulf of Gabes, **North Adr** and **South Adr** for north and south Adriatic Sea respectively, **Ion** for Ionian sub-basin, **Aeg** for Aegean Sea, **Lev** for Levantine sub-basin and **RG** for Rhodes Gyre. Major islands names are also plotted, *bal* stands for the Balearic islands, *sar* for Sardinia, *Cor* for corsica, *cre* for Crete.

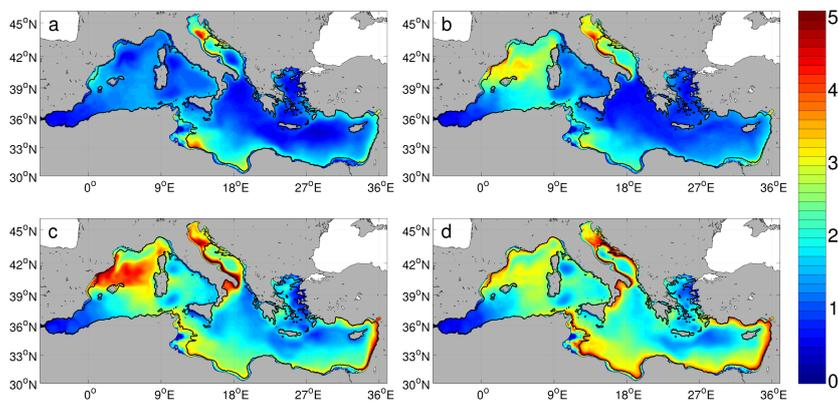


Figure 3. Modeled dissolved organic carbon inventory (mol m^{-2}) integrated over the first 100 m. Maps are averaged over the 2000-2012 period in (a) winter (Dec.-Feb.), (b) spring (Mar.-May), (c) summer (Jun.-Aug.), (d) autumn (Sept.-Nov.).

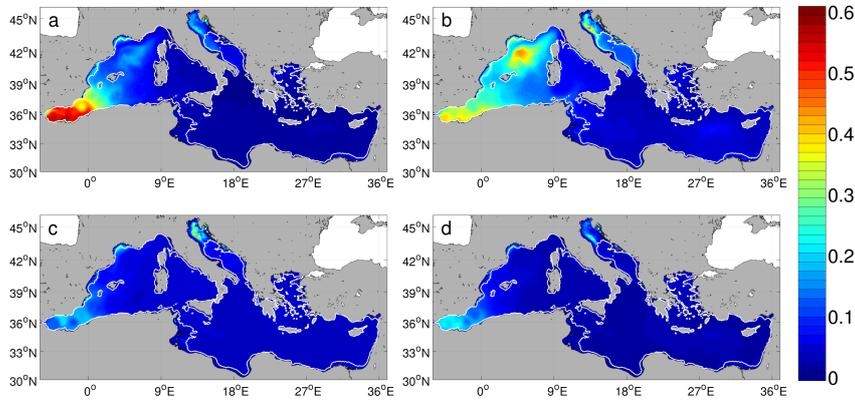


Figure 4. Modeled particulate organic carbon inventory (mol m^{-2}) integrated over the first 100 m. Maps are averaged over the 2000-2012 period in (a) winter (Dec.-Feb.), (b) spring (Mar.-May), (c) summer (Jun.-Aug.), (d) autumn (Sept.-Nov.). White lines are the 0 m and 100 m isolines.

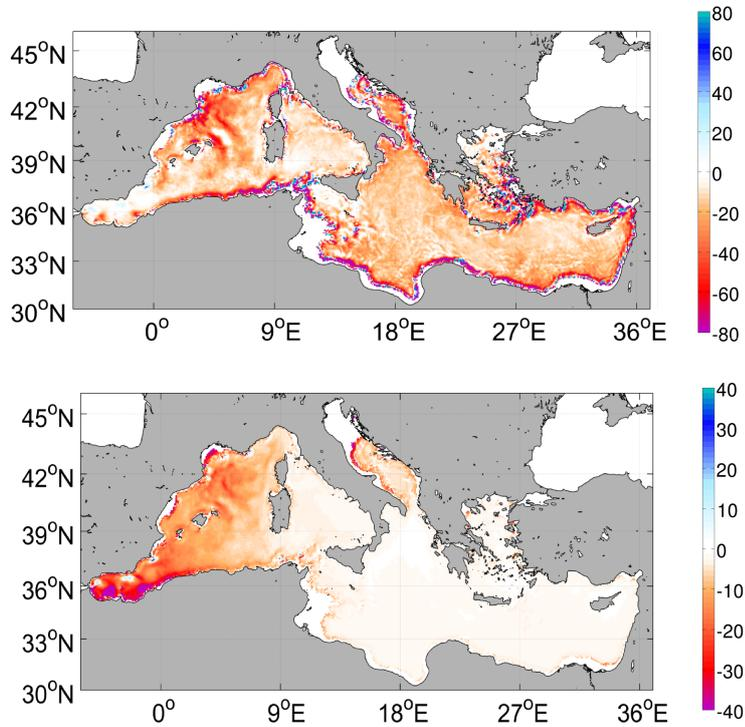


Figure 5. Maps of modeled annual DOC fluxes (top) and POC fluxes (bottom) below the 100 m layer in $\text{gC m}^{-2} \text{y}^{-1}$. Note the colorscale differences. Negative (red) means a downward flux.

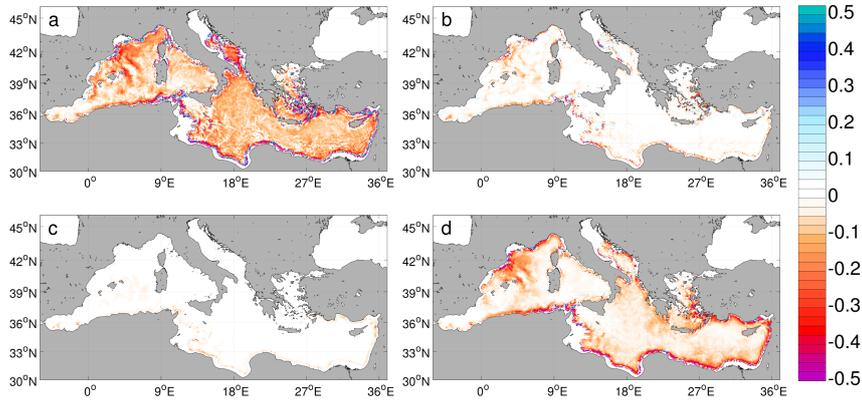


Figure 6. Maps of modeled DOC fluxes across the 100 m layer (F_{DOC}) in $\text{gC m}^{-2} \text{d}^{-1}$ in (a) winter (Dec.-Feb.), (b) spring (Mar.-May), (c) summer (Jun.-Aug.), (d) autumn (Sept.-Nov.). Negative (red) means a downward flux.

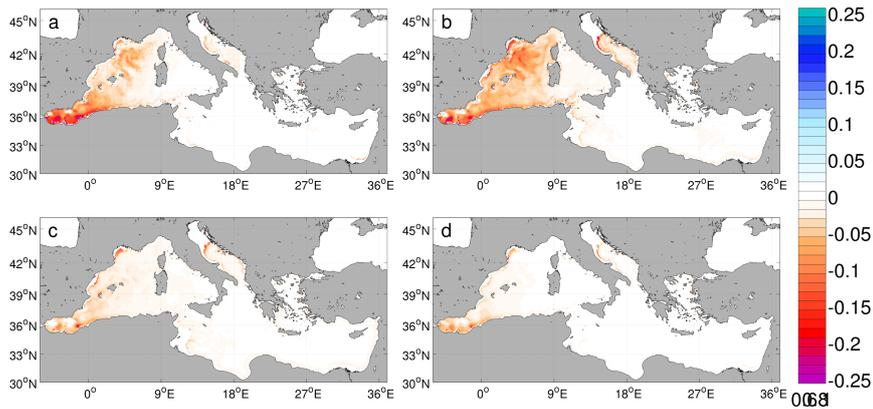


Figure 7. Maps of modeled POC fluxes across the 100 m layer F_{POC} in $\text{gC m}^{-2} \text{d}^{-1}$ in (a) winter (Dec.-Feb.), (b) spring (Mar.-May), (c) summer (Jun.-Aug.), (d) autumn (Sept.-Nov.). Negative (red) means a downward flux.

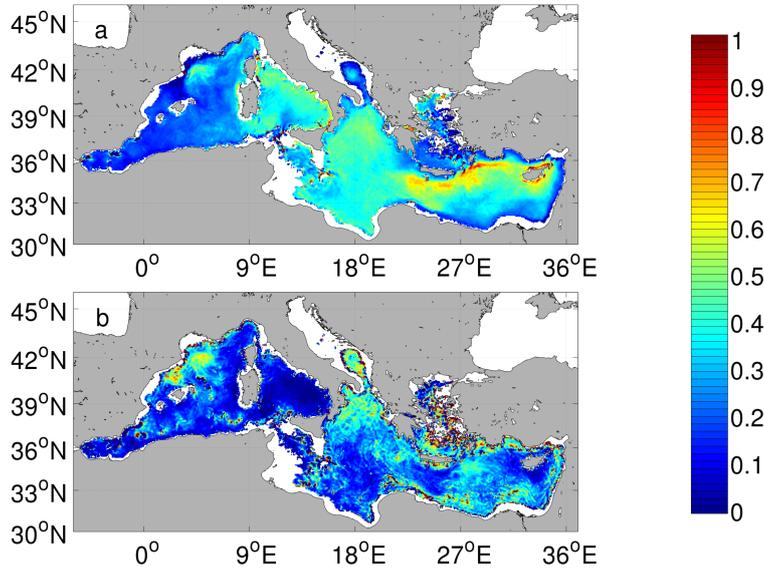


Figure 8. Ratio between export fluxes at 200 m and at 100 m (a) for POC, (b) for DOC.

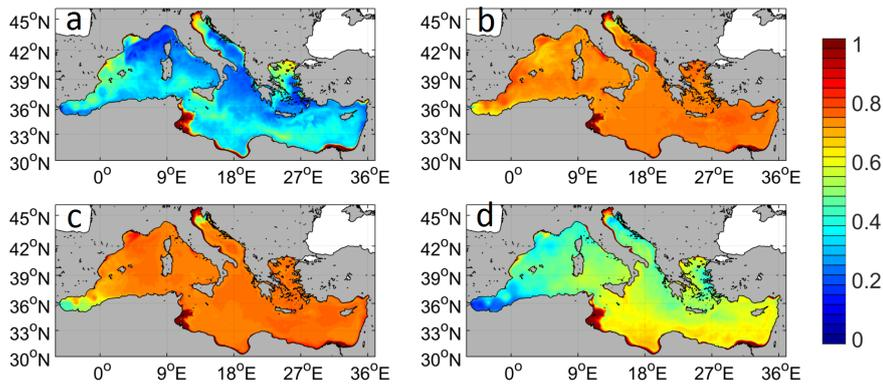


Figure 9. Seasonal variations of mean 0-50 m carbon relative quotas in small phytoplankton: (a) winter (Dec.-Feb.), (b) spring (Mar.-May), (c) summer (Jun.-Aug.), (d) autumn (Sept.-Nov.). Relative quotas are equal to 0 when the quota is minimum (i.e. when $Q_C = Q_C^{min}$) and equal to 1 when the quota is maximum (i.e. when $Q_C = Q_C^{max}$)

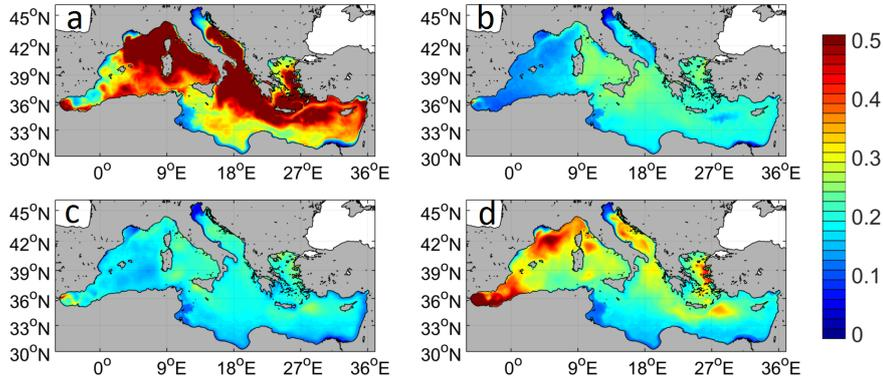


Figure 10. Seasonal variations of mean 0-50 m phosphorous relative quotas in small phytoplankton: (a) winter (Dec.-Feb.), (b) spring (Mar.-May), (c) summer (Jun.-Aug.), (d) autumn (Sept.-Nov.). Relative quotas are equal to 0 when the quota is minimum (i.e. when $Q_P = Q_P^{min}$) and equal to 1 when the quota is maximum (i.e. when $Q_P = Q_P^{max}$)

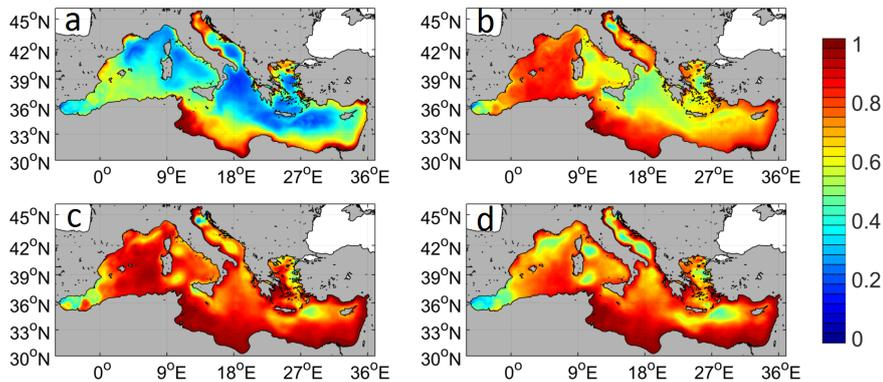


Figure 11. Seasonal variations of mean 0-50 m carbon relative quotas in bacteria: (a) winter (Dec.-Feb.), (b) spring (Mar.-May), (c) summer (Jun.-Aug.), (d) autumn (Sept.-Nov.). Relative quotas are equal to 0 when the quota is minimum (i.e. when $Q_C = Q_C^{min}$) and equal to 1 when the quota is maximum (i.e. when $Q_C = Q_C^{max}$)

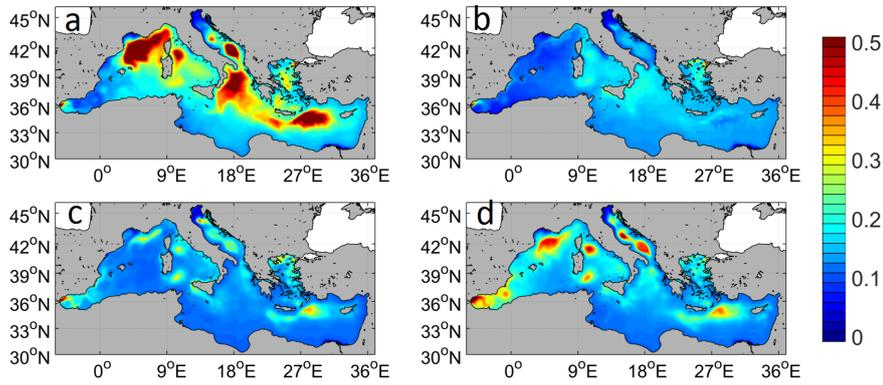


Figure 12. Seasonal variations of mean 0-50 m phosphorous relative quotas in bacteria: (a) winter (Dec.-Feb.), (b) spring (Mar.-May), (c) summer (Jun.-Aug.), (d) autumn (Sept.-Nov.). Relative quotas are equal to 0 when the quota is minimum (i.e. when $Q_P = Q_P^{min}$) and equal to 1 when the quota is maximum (i.e. when $Q_P = Q_P^{max}$)

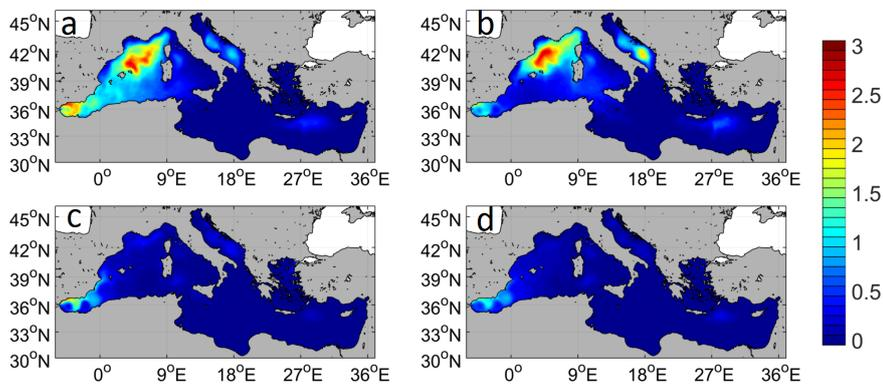


Figure 13. Seasonal variations of DOC mean 0-100 m exudation accumulated flux by large phytoplankton (in mol C.m^{-2}).

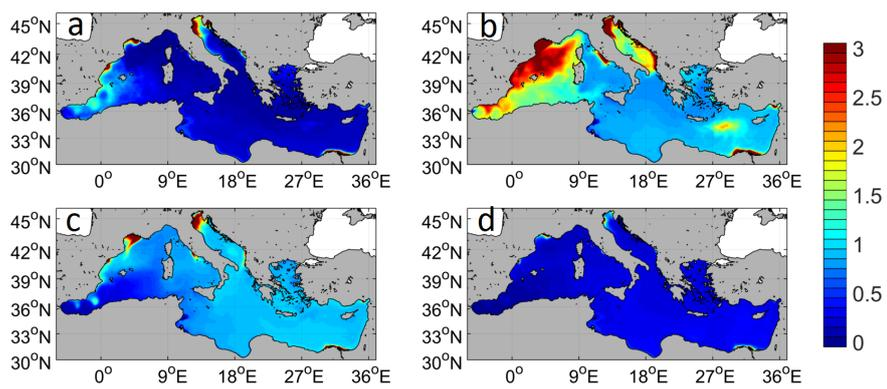


Figure 14. Seasonal variations of mDOC mean 0-100 m exudation accumulated flux by small phytoplankton (in mol C.m⁻²).